Enes Hamdi Demirci

A Master's Thesis

AGU 2023

PREPARATION AND CHARACTERIZATION OF UV CROSSLINKED ALGINATE-BASED TANNIC ACID-REINFORCED HYDROGELS

A THESIS
SUBMITTED TO THE DEPARTMENT OF BIOENGINEERING
AND THE GRADUATE SCHOOL OF ENGINEERING AND SCIENCE
OF ABDULLAH GUL UNIVERSITY
IN PARTIAL FULFILLMENT OF THE REQUIREMENTS
FOR THE DEGREE OF
MASTER OF SCIENCE

By
Enes Hamdi Demirci
June 2023

PREPARATION AND CHARACTERIZATION OF UV CROSSLINKED ALGINATE-BASED TANNIC ACID-REINFORCED HYDROGELS

A THESIS

SUBMITTED TO THE DEPARTMENT OF BIOENGINEERING

AND THE GRADUATE SCHOOL OF ENGINEERING AND SCIENCE OF ABDULLAH GUL UNIVERSITY

IN PARTIAL FULFILLMENT OF THE REQUIREMENTS

FOR THE DEGREE OF

MASTER OF SCIENCE

By

Enes Hamdi Demirci

June 2023

SCIENTIFIC ETHICS COMPLIANCE

I hereby declare that all information in this document has been obtained in accordance with academic rules and ethical conduct. I also declare that, as required by these rules and conduct, I have fully cited and referenced all materials and results that are not original to this work.

Name-Surname: Enes Hamdi DEMİRCİ

Signature :

REGULATORY COMPLIANCE

M.Sc. thesis titled PRODUCTION AND CHARACTERIZATION OF ALGINATE BASED THREE DIMENSIONAL TISSUE SCAFFOLD has been prepared in accordance with the Thesis Writing Guidelines of the Abdullah Gül University, Graduate School of Engineering & Science.

Prepared By	Advisor	Co Advisor
Enes Hamdi Demirci	Prof. Dr. Sevil Dinçer İşoğlu	Asst. Prof. Tuğrul Tolga Demirtaş

Head of the Bioengineering Program

Asst. Prof. Altan Ercan

ACCEPTANCE AND APPROVAL

M.Sc. thesis titled PREPARATION AND CHARACTERIZATION OF UV CROSSLINKED ALGINATE-BASED TANNIC ACID-REINFORCED HYDROGELS and prepared by Enes Hamdi Demirci has been accepted by the jury in the Bioengineering Graduate Program at Abdullah Gül University, Graduate School of Engineering & Science.

09/06/23

JURY:

Advisor : Prof. Dr. Sevil DİNÇER İŞOĞLU

Member : Asst. Prof. İsmail AKÇOK

Member : Prof. Dr. Sinan EĞRİ

APPROVAL:

The acceptance of this M.Sc. thesis has been approved by the decision of the Abdullah Gül University, Graduate School of Engineering & Science, Executive Board dated ….. /….. / …….. and numbered ……..……. .

…….. /…….. / ……..

(Date)

Graduate School Dean
Prof. Dr. İrfan ALAN

ABSTRACT

PREPARATION AND CHARACTERIZATION OF UV CROSSLINKED ALGINATE-BASED TANNIC ACID-REINFORCED HYDROGELS

Enes Hamdi Demirci
MSc. in Bioengineering
Advisor: Prof. Dr. Sevil Dinçer İşoğlu
co-Advisor: Asst. Prof. Tuğrul Tolga Demirtaş

June 2023

Alginate is a commonly used biopolymer in bioprinting applications. However, alginate-based bioinks have some mechanical limitations for printing purposes. Also, existing methacrylation methods are time consuming and have low methacrylation efficiencies. Based on these facts, we focused on enhancing mechanical strength of alginate within the scope of this thesis. To do this, we applied microwave irradiation during methacrylation process of alginate and compared the efficiencies between conventional and microwave irradiation. Here, we report a significantly faster and more effective method for the controlled synthesis of methacrylated alginate (Alg-MA) by microwave energy (250 W) with approximately 80% degree of methacrylation (DM) even with a very low amount of metyhacrylation agent (aminoethyl methacrylate (AEMA)). Rheological and mechanical analyses showed that Alg-MAs synthesized by microwave irradiation allowed the formation of more elastic and stronger hydrogels with very high stability than the ones synthesized by the conventional method. Additionally, we combined these hydrogels with tannic acid by a second cross-linking in order to improve their mechanical strength and tissue integration ability. Addition of TA provided hydrogels very good mechanical strength and also antibacterial characteristics towards gram-positive and gram-negative bacteria. As a conclusion, hydrogels with mechanically superior properties and antibacterial characteristics were obtained by MW-assisted methacrylation and physical cross-linking by TA.

Keywords: alginate, microwave, bioink, tannic acid, hydrogels.

ÖZET

IŞIK İLE ÇAPRAZ BAĞLANABİLEN ALJİNAT BAZLI TANNİK ASİT İLE GÜÇLENDİRİLMİŞ BİYOMÜREKKEP HİDROJELLERİN HAZIRLANMASI VE KARAKTERİZASYONU

Enes Hamdi Demirci
Biyomühendislik Anabilim Dalı Yüksek Lisans
Tez Yöneticisi: Prof. Dr. Sevil Dinçer İşoğlu
Tez Yöneticisi II: Dr. Öğr. Üyesi Tuğrul Tolga Demirtaş

Haziran-2023

Aljinat biyobaskı uygulamalarında yaygın bir şekilde kullanılan bir biyopolimerdir. Fakat, aljinat bazlı biyomürekkeplerin baskı amaçları için bazı mekanik sınırlamaları mevcuttur. Ayrıca, mevcut metakrilasyon yöntemlerinin zaman alması ve metakrilasyon derecesinin düşük olması gibi sınırlamaları bulunmaktadır. Buradan hareketle, tez çalışması kapsamında aljinatın mekanik özelliklerinin iyileştirilmesi üzerine odaklanılmıştır. Bu amaçla, metakrilasyon işlemi mikrodalga enerjisi uygulanarak gerçekleştirilmiş ve geleneksel ile mikrodalga uygulamasının verimleri kıyaslanmıştır. Çalışmada, 250 W mikrodalga enerjisi uygulanarak, çok düşük metakrilatlama ajanı varlığında (AEMA) %80 metakrilatma derecesine sahip aljinat sentezi için hızlı ve etkin bir yöntem ortaya konmuştur. Reolojik ve mekanik analizlere göre, mikrodalga ile sentezlenen aljinatların geleneksel yöntemle sentezlenenlere göre daha elastik ve güçlü oldukları gözlenmiştir. Ayrıca, daha üstün mekanik özellikler ve doku entegrasyonu kabiliyetine sahip hidrojeller elde etmek amacıyla bunlar tannik asit ile etkileştirilmişler ve ikincil çapraz bağlanma ile mekanik gücün arttığı gözlenmiştir. Buna ek olarak, tannik asit etkisi ile hidrojellerin antimikrobiyal özellik kazandığı görülmüştür. Sonuç olarak, mikrodalga ve TA yardımıyla, üstün mekanik özelliklerde ve antimikrobiyal karakterde aljinat hidrojeller elde edilmiştir.

Anahtar kelimeler: Aljinat, mikrodalga, biyomürekkep, tannik asit, hidrojeller

Acknowledgements

I would like to express my gratitude to my supervisor Prof. Dr. Sevil DİNÇER İŞOĞLU and my co-advisor Asst. Prof. Tuğrul Tolga DEMİRTAŞ for their support, patience and guidance throughout my thesis study.

I would like to thank TUBITAK for the support within the scope of BIDEB 2210-C Graduate Student Scholarship Program and TUBITAK 222M325.

I would like to express my special thanks to my laboratory mates Nazende Nur BAYRAM and Seray ZORA TARHAN for their support in the experimental parts of my thesis study.

I would also like to thank my dear friends Aylin Saniye CEYLAN and Özgür Kaan ÜNAL for their support and motivation.

Finally, I would like to express my endless thanks to my family; my father Köksal DEMİRCİ, my mother Rabiye DEMİRCİ, my sister Meltem KULAK and my nephew Mehmet KULAK, the new member of our family, for their support throughout my life.

TABLE OF CONTENTS

LIST OF FIGURES

LIST OF TABLES

To My Family

Chapter 1

1.Introduction

1.1. Tissue Engineering

Tissue and organ transplantation have been life-saving procedures for millions of people worldwide suffering from various diseases, including organ failure, severe burns, and cancer. However, the shortage of suitable donor organs, tissue rejection, and the risks of infections and complications associated with transplantation have highlighted the need for alternative approaches [1–3]. The tissue engineering (TE) approach is promising for mimicking or developing various biological structures suitable for the mentioned purpose.

TE is an interdisciplinary field that combines knowledge from engineering, life science, and material science to develop biological substitutes that can repair or develop tissue function [4]. These biological substitutes, often called scaffolds, are made of biocompatible materials, and are also a critical component of tissue engineering, as they supply a three-dimensional structure for cells to grow and differentiate, and can also act as a delivery system for growth factors and other signalling molecules that are necessary for tissue development and regeneration. Cells are often seeded onto or within the scaffold, where they can proliferate and differentiate into the desired tissue type. The resulting tissue construct can then be transplanted into the body to replace damaged or diseased tissue.

TE and regenerative medicine (RM) strategies aim to repair or replace damaged tissues or organs using engineered constructs composed of cells, biomaterials, and biochemical signals. To achieve successful tissue integration and regeneration, it is necessary to interact and integrate with the surrounding tissues and cells, and to

incorporate appropriate physical and cellular signals that can promote tissue growth, differentiation, and function [5].

To promote tissue regeneration and influence cell behaviour, one approach is to incorporate biologically active proteins such as growth factors, cytokines, and extracellular matrix (ECM) proteins into the 3D printing process. Additionally, the inclusion of DNA can also aid in achieving this goal. For example, growth factors such as bone morphogenetic protein (BMP) and transforming growth factor-beta (TGF-beta) can promote cell proliferation, differentiation, and ECM production in bone and cartilage tissue engineering. Similarly, DNA-based technologies such as gene therapy can be used to introduce new genes into the cells, which can alter their behaviour and promote tissue growth [6]. In addition to these modifying factors, other factors such as mechanical stimulation, cell alignment, and nutrient supply are also crucial for successful TE and regeneration [5, 6].

In summary, the incorporation of modifying factors such as DNA and biologically active proteins is crucial for the advancement of TE and RM approaches, as it enables the creation of functional tissues and organs that can effectively treat various diseases and injuries. Therefore, the design and implementation of TE and RM strategies require a multidisciplinary approach that integrates knowledge from diverse fields such as biology, engineering, and the science of materials.

However, current tissue engineering strategies have some limitations, such as the need for a better understanding of cell biology and the complex interactions between cells and biomaterials, the need for better biomaterials with suitable mechanical and biological properties, and the need for more efficient methods for growing and expanding cells [6, 7]. In order to overcome the limitations and imitate the complex structure of tissue, it has been focused on obtaining more automated and reproducible systems with three-dimensional printing technology, including biological components [8, 9].

1.2. 3D Printers & Bioprinters for Tissue Engineering

David E. H. Jones first proposed the concept of 3D printing in a paper he wrote in 1974, titled "A Three-Dimensional Cartesian Coordinate Positioning System." [10]. However, it was Hideo Kodama who first developed a functional prototype of a 3D printing system using photopolymerization in 1981 [11]. After that, Charles W. Hull, in 1984, developed the first three-dimensional printing objects by stereolithography (SLA) (Figure 1.1) [12]. Then, since its origin in the 1980s, additive manufacturing or 3D printing technology has made significant progress, and it is now being used in various industries, including medicine, aerospace, automotive, and architecture, among others. Because Kodama's work laid the groundwork for developing various additive manufacturing processes widely used today. Furthermore, bioprinting technology is the most up-and-coming application in the field of 3D printing, where it has the potential to revolutionize TE and RM [13].

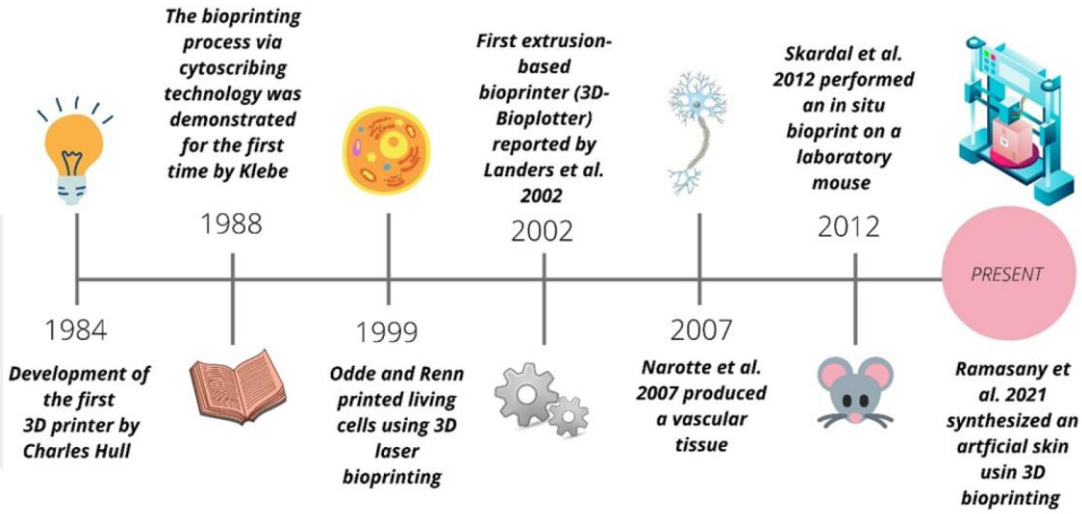

Figure 1.1 Evolution of the 3D bioprinting technology [12, 14, 15]**.**

Both technologies (3D printing/bioprinting) use layer-by-layer fabrication processes from CAD models, but the difference between the two lies in the materials used. A range of materials such as plastics, metals, and ceramics are used to form objects in 3D printing. These materials are not living and do not contain any biological components. In contrast, 3D bioprinting involves the use of bioinks that consist of

living cells and biomaterials, such as hydrogels, that can support cell growth and differentiation [16–23].

The goal of 3D bioprinting is to create functional tissue constructs that can be utilized for TE, RM, and drug discovery applications [18]. 3D bioprinting offers many potential benefits over traditional tissue engineering techniques. Firstly, by using bio-inks that contain living cells and bioactive molecules, it enables the creation of intricate tissue structures that can mimic the natural architecture of tissues and organs in the body instead of using traditional methods. Secondly, it allows the precise control of mechanical properties, which can be adapted to meet the specific requirements of the tissue being engineered. Thirdly, it offers a faster and more efficient method of tissue fabrication, as the entire process can be automated, reducing the need for manual labor [24–26]. Furthermore, 3D bioprinting techniques enable the creation of patient-specific scaffolds based on anatomically accurate 3D models generated from medical imaging data. This ensures that the scaffold is tailored to the unique requirements of the patient's tissue defect, thereby improving the success rate of tissue regeneration and reducing the risk of rejection or adverse reactions. The process of additive manufacturing involves the use of computer-aided design (CAD) software to create a digital model of the tissue structure. This digital model is then turned into a series of thin, horizontal slices, which are used as a guide for the printer. The printer then builds the tissue structure layer by layer, depositing the material in a controlled manner. This process is able to repeat itself multiple times until the desired tissue structure is created [27]. These constructs can be utilized for different purposes, such as modeling diseases, screening drugs, and even RM. The use of cell-laden bio-inks enables the creation of more complex and functional tissue constructs, as the cells can differentiate and organize themselves within the construct to form functional tissue. On the other hand, 3D printing can be utilized for lots of applications, for example, prototyping, manufacturing, and product design. It is typically used to create solid objects with complex geometries that may be difficult or impossible to fabricate using traditional manufacturing techniques [23, 26]. However, it is not typically used for biological applications, as it does not involve the use of living cells or biomaterials that can promote tissue formation and cell growth. In general, while both technologies have their unique applications, 3D bioprinting is still in its initial stages of development in tissue engineering. The use of 3D bioprinting has the possibility of

bringing a significant change to the medical field. It can allow the production of customized tissues and organs that are specifically designed for each patient, leading to advancements in disease modeling and drug development. Ultimately, this technology can provide a ray of hope to individuals who are struggling with various medical conditions [26].

1.2.1. 3D Bioprinting Process

The 3D bioprinting process generally involves the following steps (Figure 1.2) [12]:

- 3D scanning of the required organ or tissue: To initiate the bioprinting process, medical imaging data of the tissue or organ that requires printing is collected using techniques such as CT scans or MRIs. The data is then processed and converted into a 3D digital model.
- 3D bio-modelling of the required tissue or organ geometry: Based on the 3D digital model, a virtual 3D bio-model is created using specialized software. This helps to determine the geometry and structure of the tissue or organ that needs to be printed.
- Formulation of bio-inks from cellular or cell-free biomaterials: The ink formulation is a critical step in the bioprinting process. Biomaterials, such as hydrogels, are combined with cells to create a bioink that can be used for bioprinting.
- Three-dimensional bioprinting (calibration and slicing): The bio-ink is loaded into a bioprinter, which then deposits the ink layer by layer, based on the 3D bio-model. The printer is calibrated to ensure accuracy and precision during printing. The bio-ink is sliced into layers to enable precise deposition of the ink.
- Maturation: After bioprinting, the printed structure is left to mature and grow. This enables the cells to proliferate and differentiate, leading to the formation of tissue or organ-like structures.
- Physical, chemical, and biological characteristics and potential applications of the bio-printed structure: The final step involves analyzing the bio-printed structure to ensure that it meets the required specifications. This involves testing the structure for mechanical properties, cell viability, and functionality.

In summary, the 3D printing process has revolutionized manufacturing and allowed for the creation of complex and intricate structures that would be difficult or impossible to produce utilizing conventional manufacturing methods [13, 28, 29].

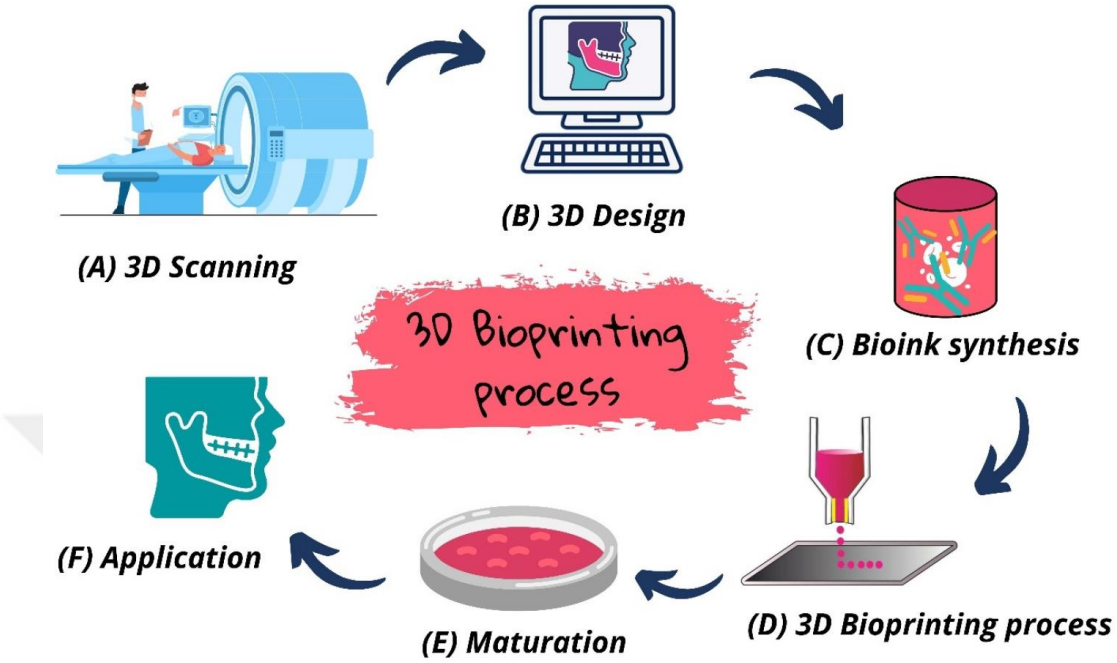

Figure 1.2 Phases of the 3D bioprinting operation [12].

1.2.2. Types of 3D Bioprinting

3D bioprinting is an emerging technology that enables the production of complex 3D structures with living cells and the fields of tissue engineering and regenerative medicine have shown a lot of interest in 3D bioprinting. [13]. While bioprinting has made significant strides in recent years, there is still no single bioprinting technique that can produce all the scales and complexities of synthetic tissues [17]. 3D bioprinting technologies can be broadly classified into three main types based on their working mechanisms: inkjet bioprinting, laser-assisted bioprinting, and extrusion-based bioprinting [30].

In order to obtain optimal outcomes in 3D bioprinting, it is crucial to take into account various factors, such as the printing precision, the survival rate of the cells, and the choice of the material for creating the desired 3D structures. Other factors to consider include the biocompatibility of the materials, the mechanical properties of the printed structures, and the ability to vascularize the printed tissues or organs [13].

Besides, these methods have some limitations as well as advantages, and researchers continue to investigate and develop new bioprinting techniques and materials to improve these shortcomings, including the printing precision, the survival rate of the cells, and the ability to print complex structures. Additionally, the choice of method depends on the specific application and the type of biomaterial being printed [26].

1.2.2.1. Inkjet-Based Bioprinting (IBB)

IBB is a type of 3D bioprinting technology that allows for the printing of live cells and biomaterials in a precise and controlled manner. It works by using an inkjet printer to deposit tiny droplets of a cell-loaded hydrogel onto a substrate, which can be a tissue culture dish, a scaffold, or even a living organism [31].

The use of IBB in tissue engineering (TE) and regenerative medicine (RM) has many potential applications. For example, it could be used to create artificial organs or tissues for transplantation or to develop new drugs and therapies. IBB also permits accurate positioning of cells, which can be important in creating complex tissue structures [32]. IBB has a lot of advantages such as low cost, non-contact nature, reduced risk of contamination, and the ability to achieve high resolution and precision as well [33]. Certain studies have been successful in printing droplets containing only one cell. This level of precision can be important in creating tissues with specific structures and functions.

The process of IBB involves several steps. First, the cells are suspended in a hydrogel solution that provides a supportive and nourishing environment for the cells. The hydrogel solution is then loaded into the ink cartridge of an inkjet printer, which is specially adapted to handle the viscous nature of the hydrogel. The printer then ejects droplets of the hydrogel solution onto the substrate using either thermal or piezoelectric methods, as represented in Figure 1.3 [34, 35]. Thermal inkjet printers work by heating a tiny resistor located in the printhead, which causes a small amount of ink to vaporize and form a bubble [36]. This bubble rapidly expands, pushing the ink droplet out of the nozzle. Piezoelectric inkjet printers use an electric charge to create a vibration in a tiny crystal, which then ejects a droplet of ink [37]. As the droplets are deposited onto the substrate, they begin to solidify, creating a 3D structure. Because of the hydrogel's nourishing and protective environment, the cells

within the droplets continue to be alive and viable. With 3D bioprinting, it is possible to fabricate intricate tissues and organs that have diverse uses, such as regenerative medicine, tissue engineering, and drug development.

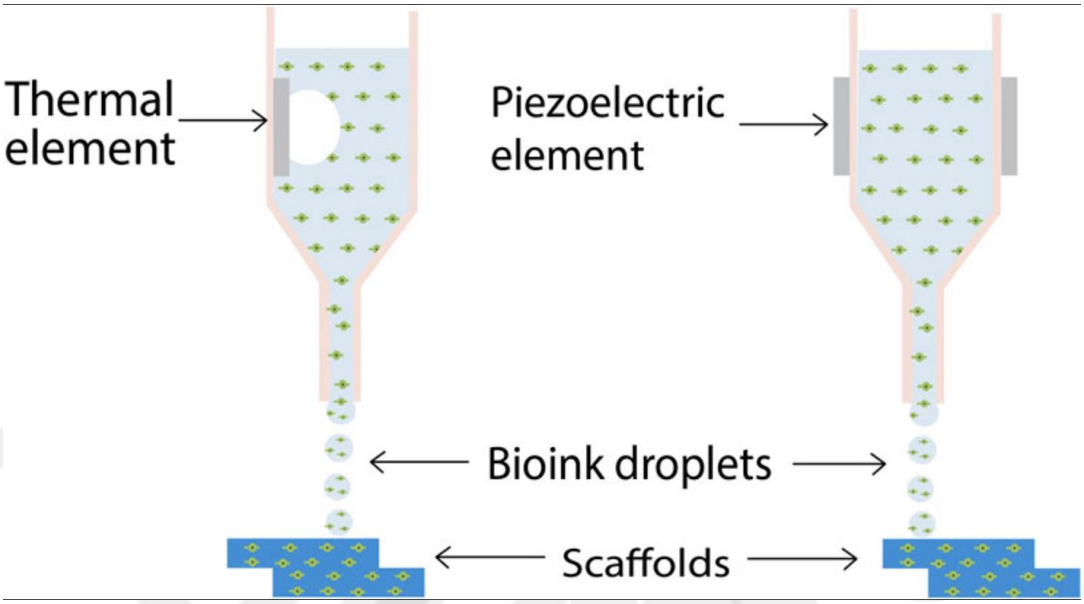

Figure 1.3 Inkjet bioprinting [31]**.**

Tse et al. utilized a printer that uses piezoelectric technology to deposit ink in order to create neural tissue from porcine Schwann cells and neuronal NG 108-15 cells [38]. They found that the viability of both neuronal and glial cells was high immediately after printing, with 86% and 90% respectively. Additionally, the proliferation rate of the printed cells was similar to that of non-printed cells. After 7 days, the printed cells had developed neurites that elongated, which is a positive sign of neural tissue formation. This study showcases the possibilities and capabilities of bioprinting technology to create complex tissues, such as neural tissue, for use in regenerative medicine and tissue engineering.

IBB is still a relatively new technology, and there are many challenges that still need to be addressed, such as improving cell viability and ensuring the precise placement of cells within the printed structure. However, it holds great promise for the future of TE and RM, and it is expected that IBB will become increasingly significant in the creation of novel treatments and therapies for various ailments and illnesses.

1.2.2.2. Laser-Based Bioprinting (LBB)

LBB is a type of 3D bioprinting technique and in this technique, laser-assisted 3D bioprinter technology makes use of a pulsed laser beam so as to deposit bio-ink-containing living cells onto a substrate with high precision and accuracy, as seen in figure 4 [39]. The laser radiation used in this technique is highly monochromatic, meaning that it consists of only one wavelength of light, and it is focused and coherent, meaning that it is well-aligned and produces a tightly focused beam [40]. The laser beam is focused onto the bio-ink, causing it to rapidly heat and expand, which generates a small droplet of the ink [41]. These droplets are then precisely deposited onto the substrate to form a 3D pattern of living cells. The laser beam is pulsed to avoid heating or damaging the cells and to ensure the bioink is deposited accurately.

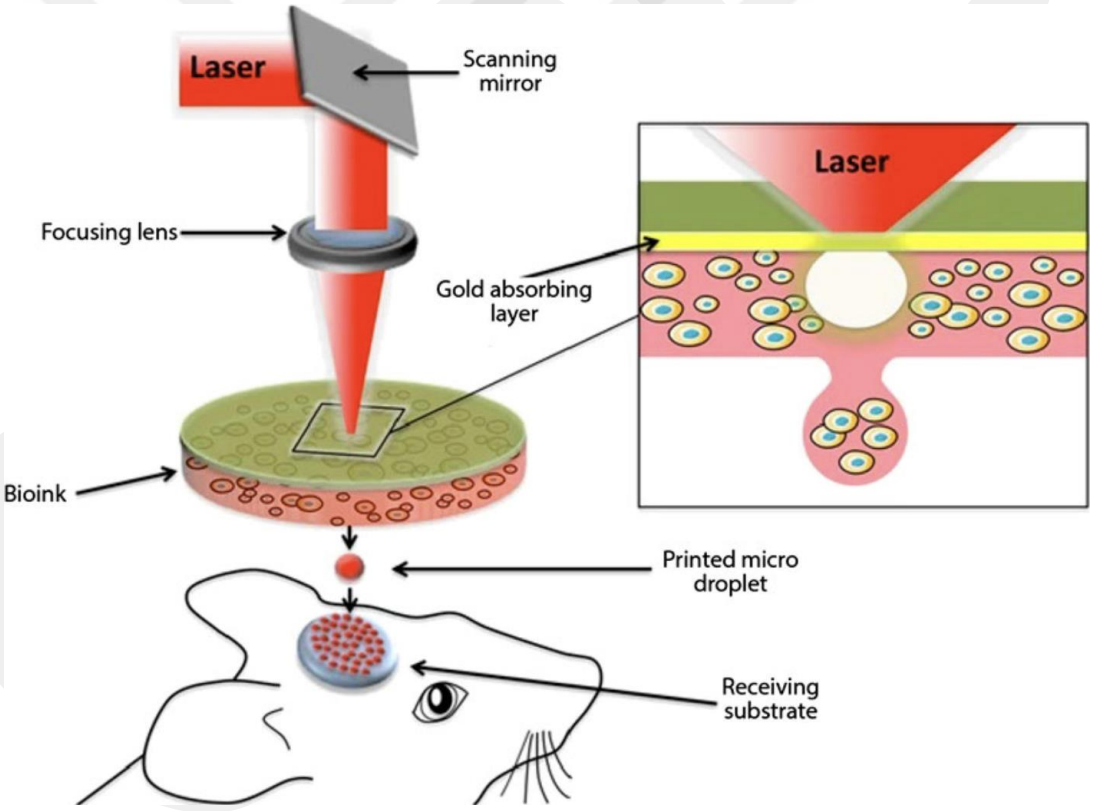

Figure 1.4 Laser-assisted bioprinting [42]**.**

LBB has the capability to transform the field of tissue engineering and regenerative medicine by facilitating the production of intricate and fully functional tissues and organs, such as synthetic skin, cartilage, and blood vessels. It is also being investigated for drug screening and toxicology testing. It offers many advantages over traditional tissue engineering techniques, including high precision, scalability, and the

ability to print multiple cell types and materials simultaneously [43, 44]. Additionally, it minimizes damage to the cells and extracellular matrix during printing, which is vital for maintaining cell viability and function.

However, many challenges must be overcome before LBB can be widely adopted in clinical settings. These include improving the viability of the printed cells, optimizing the printing parameters, and ensuring the safety and biocompatibility of the materials used in the process.

1.2.2.3. Extrusion-Based Bioprinting (EBB)

Rapid prototyping (RP), also known as additive manufacturing or 3D printing, is the process of creating physical models or prototypes of a design using 3D computer-aided design (CAD) data [45]. It involves the layer-by-layer deposition of materials, such as polymers, metals, or ceramics, to build up a three-dimensional object [46]. RP is also referred to as solid freeform fabrication because it allows for the creation of complex geometries and internal architectures that may not be possible with traditional manufacturing techniques. RP has found extensive use in diverse areas, such as product development, engineering, and biomedical applications, including medical device design and tissue engineering [47, 48]. In the medical field, rapid prototyping is used to create customized implants, prosthetics, and other medical devices. It can also be used to create models of organs, tissues, and other structures for surgical planning and training. The ability to create complex, customized objects quickly and easily has made rapid prototyping an important tool in many industries. It has opened up new possibilities for design and manufacturing, allowing for faster iteration and testing of new ideas [49].

EBB is one of the most popular and promising techniques for fabricating 3D tissue constructs due to its unique advantages. EBB enables the precise deposition of bio-inks in a layer-by-layer manner to create complex 3D tissue constructs that mimic the native tissue architecture [50].

EBB offers the crucial benefit of enabling the deposition of a high concentration of cells, providing greater flexibility in the selection of materials with varying cell densities and viscosities. As a result, EBB is a highly versatile and customizable technique that can be adapted to various tissue types. EBB can also provide enhanced structural support for printed components when using high-viscosity materials.

Additionally, EBB has the advantage of creating a better environment for preserving cell viability and function in cases where low-viscosity materials are used [51]. EBB also offers several advantages over other bioprinting techniques. For example, it can print at higher speeds, which facilitates scalability, and the process-induced cell damage is relatively less compared to other techniques [52]. Additionally, EBB allows for the use of multiple printing heads, enabling the use of multiple bio-inks to fabricate more complex tissue structures.

However, maintaining cell viability during the extrusion bioprinting process can be challenging. The extrusion pressure and nozzle gauge can affect cell viability, with higher pressures and smaller gauge sizes leading to lower cell viability. This is because the mechanical forces generated during the printing process can damage or kill the cells [34]. In order to improve cell viability during extrusion bioprinting, several strategies have been proposed, including optimizing the printing parameters (such as extrusion pressure, nozzle size, and printing speed), incorporating protective agents in the bio-ink (such as antioxidants, growth factors, and ECM proteins), and using pre-culture techniques to enhance the robustness of the cells.

Furthermore, the bio-inks used in EBB can be crosslinked using different mechanisms like ionic, thermal, or photocrosslinking, making them more stable and durable, as seen in Figure 1.5. The use of crosslinking agents also allows for the fabrication of free-standing 3D structures that can be used for implantation [7].

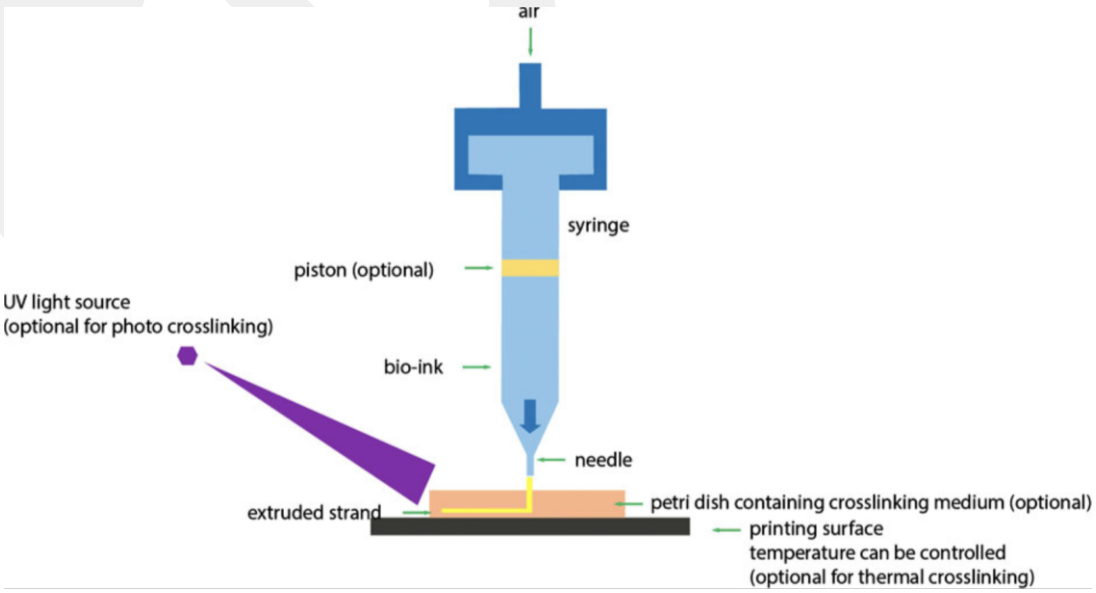

Figure 1.5 Extrusion-based bioprinting [49]**.**

Tan et al. demonstrated the application of the multi-nozzle EBB to creating tubular structures made of alginate through 3D bioprinting. The researchers explored the impact of varying the viscosity of the alginate solutions on the final printed structures [53]. The study demonstrated that the extrusion-based bioprinting technique can be used to fabricate large-diameter vascularized constructs. The results indicated that the printing parameters, including the nozzle diameter, the printing speed, and the viscosity of the alginate solution, significantly affect the mechanical properties and morphology of the printed structures. The findings of this study hold significance in the fields of tissue engineering (TE) and regenerative medicine (RM), as they offer a promising approach for the fabrication of large-diameter vascularized constructs that can be used for the replacement or regeneration of damaged tissues and organs.

Dolati and colleagues conducted a study on using coaxial bioprinting to create a vascular conduit made of alginate [54]. The study aimed to develop a bioprinting technique that could create vascular conduits with enhanced mechanical properties, which could potentially be used in regenerative medicine. The researchers applied the same bioprinting technique to incorporate micro-engineered blood vessels and cellular layers into the extracellular matrix of target tissues, thus demonstrating the potential for tissue engineering applications.

Across the board, EBB is a highly versatile and promising technique for fabricating 3D tissue constructs with excellent accuracy and precision, which makes it a valuable tool for TE and RM.

Despite the benefits offered by additive manufacturing for tissue engineering, there are still obstacles that need to be addressed. One challenge is the need for suitable biomaterials that can be printed with high accuracy and resolution [26].

1.3. Bio-Inks

Bio-inks utilized in 3D bioprinters are vital components for the 3D bioprinting process [55, 56]. Bio-inks are formulations containing cells, biomolecules, and a scaffold material that can be used in bio-fabrication techniques such as 3D bioprinting, to create complex 3D tissue structures [57]. These formulations are designed to simulate the hydrated environment of natural tissues, which is essential

for maintaining cell viability and proliferation [58]. Bio-inks can be made from various materials, including hydrogels, which are highly hydrated networks of cross-linked polymers that can hold large amounts of water. Hydrogels are a popular choice for scaffold materials in bio-inks due to their ability to mimic the extracellular matrix of natural tissues and provide a highly hydrated environment for the cells [59, 60]. The term "bio" in bio-inks refers to the fact that the formulation contains living cells, which are the true biological components of the material [61, 62]. A 3D-printed tissue construct can be created by combining a polymer solution and cells, which are then printed into a specific shape. A crosslinker is added to the polymer solution to create stability. Once the mixture is printed, it is exposed to UV light, which causes the crosslinker to bond and solidify the structure of the tissue construct. This can be used in a variety of applications, such as implanting engineered tissue into a patient, using the construct for drug screening, or creating organ models on microfluidic systems (Figure 1.6).

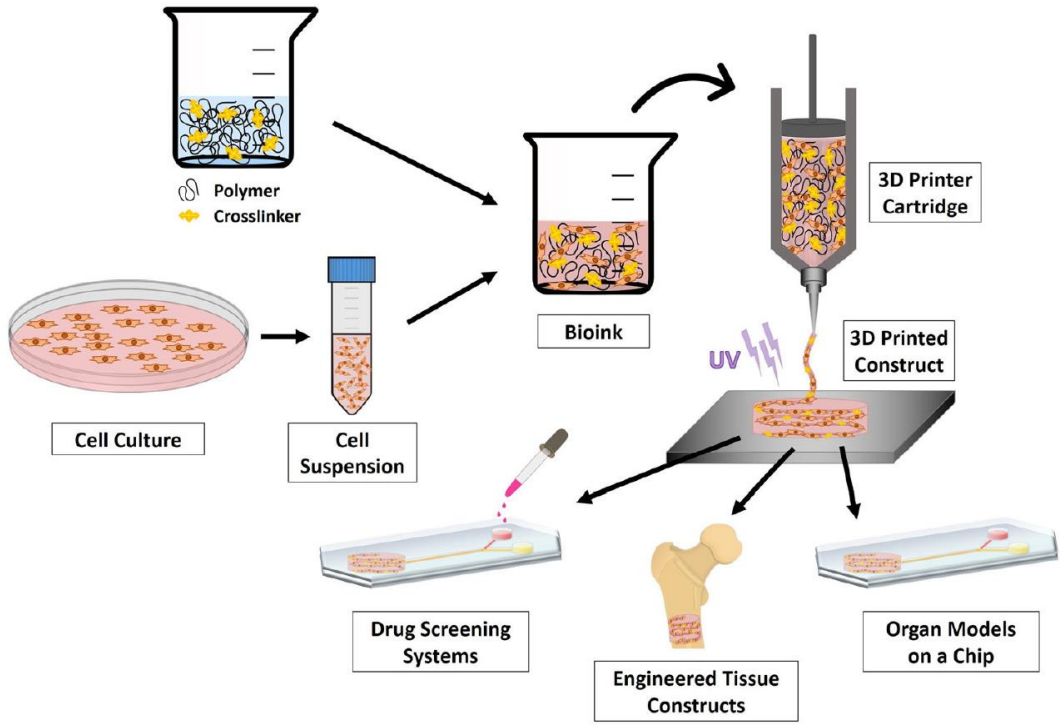

Figure 1.6 The process of creating a 3D printed tissue structure, along with its various uses and applications [63]**.**

By using bio-inks, researchers can create tissue models that closely mimic natural tissues in terms of their cellular organization, mechanical properties, and other characteristics. Bio-inks are an important tool for tissue engineering and regenerative

medicine, as they allow researchers to create complex tissue models that can be used for drug screening, disease modelling, and other applications. In addition, bio-inks can be customized to incorporate specific cell types or biomolecules, allowing researchers to create tissue models that are tailored to their specific research needs.

1.3.1. Critical Properties of Bio-Inks

Hydrogels are commonly used as bio-inks for the 3D printing of tissue-engineered constructs due to their unique properties, such as their ability to absorb large amounts of water and their ability to mimic the extracellular matrix (ECM) of natural tissues. However, hydrogels used as bio-inks must possess certain essential properties to ensure their effectiveness in 3D printing applications [64, 65].

A brief overview of each of these crucial properties:

1. Biocompatibility:

Biocompatibility is an important property of hydrogels used as bioinks, as they will be in direct contact with living cells and tissues. The hydrogel must not cause any adverse reactions when it comes into contact with living cells or tissues. The hydrogel should support cell adhesion, proliferation, and differentiation [59, 66].

2. Printability:

Printability is another crucial property, as it determines the ability of the hydrogel to be extruded from the 3D printer nozzle and maintain its shape during printing. The hydrogel should be able to flow through a printer nozzle, maintain its shape during the printing process, and solidify quickly once it is deposited on the printing substrate [34, 67].

3. Mechanical Property:

Mechanical properties such as stiffness, elasticity, and toughness are also important as they can affect the structural integrity and functionality of the printed tissue-engineered constructs. The hydrogel should have the appropriate mechanical strength and stiffness to support the cells and tissues being printed. The mechanical properties should match the properties of the target tissue [59, 68].

4. Hydrophilicity:

Hydrophilicity is another essential property of hydrogels used as bio-inks, as it determines the ability of the hydrogel to absorb and retain water, which is important for maintaining cell viability and facilitating nutrient and waste exchange. The hydrogel should have a high water content and be able to absorb and retain water, which is necessary for the growth and survival of cells [67, 69].

5. Geometric Structure:

The geometric structure of the hydrogel can also influence the behaviour of cells within the printed construct. The hydrogel should be able to form complex three-dimensional structures that mimic the architecture of natural tissues [34, 52].

6. Biodegradability:

Biodegradability is an important property for hydrogels used as bioinks, as they need to degrade over time and be replaced by newly synthesized tissue. The hydrogel should be able to degrade over time, allowing the cells and tissues to grow and mature, and eventually replace the scaffold [70, 71].

Incorporating guidance cues, such as morphogens, growth factors, and topography can further enhance the properties of the hydrogel-based scaffolds. Topography can guide cell behaviour and promote cell alignment and tissue formation. Growth factors and morphogens can regulate cell proliferation, differentiation, and tissue development [34].

1.4. Natural and Synthetic Biomaterials for 3D Bioprinting

3D bioprinting involves the use of materials that are able to mimic the features of living tissues in order to create functional constructs [72]. The biomaterials utilized for the production of bio-inks should have some characteristics such as biocompatibility, printability, and biodegradability. Selecting the right biomaterials is critical for ensuring the safety and efficacy of 3D bioprinting applications in tissue engineering, regenerative medicine, and drug discovery [73]. The biomaterials used in 3D bioprinting can be broadly classified into two categories: natural polymers and synthetic polymers [74–76].

Natural polymers, particularly in hydrogel form, offer several benefits when it comes to creating a convenient microenvironment for encapsulated cells [73]. Hydrogels refer to networks of hydrophilic polymer chains that exist in three dimensions and are capable of absorbing significant amounts of water without losing their shape or structure. This property makes hydrogels particularly attractive for use as cell encapsulation matrices, as they can create a supportive and nurturing environment for the encapsulated cells [67].

Hydrogels possess the advantage of being biocompatible, implying that they can be employed in various biomedical applications without causing any harmful effects on live cells. Additionally, natural polymers, such as collagen, gelatine, alginate, and chitosan, are attractive materials for cell encapsulation due to their biocompatibility, biodegradability, and similarity to the extracellular matrix (ECM) found in living tissues [77]. The ECM is a sophisticated system of proteins and polysaccharides that offer structural support and chemical signals to cells, and natural polymers can mimic some of these properties. Encapsulating cells within a hydrogel can protect them from harsh external conditions, such as shear stress, changes in pH or temperature, and immune responses [68]. The hydrogel can also serve as a physical barrier to prevent the cells from migrating and forming unwanted tissue structures. Additionally, hydrogels can be modified to provide cues that promote cell growth and differentiation, and making them an excellent choice for use in tissue engineering.

Broadly, natural polymers in the form of hydrogels offer several advantages when it comes to providing a favourable microenvironment for encapsulated cells [78]. Their biocompatibility, ability to mimic the ECM, protection of encapsulated cells, and biodegradability make them an excellent choice for various biomedical applications, including tissue engineering, drug delivery, and regenerative medicine.

On the other hand, synthetic polymers are macromolecules that are created through chemical synthesis, rather than being naturally occurring [7, 79]. Polyethylene glycol (PEG), polycaprolactone (PCL), poloxamers (Pluronic), polypropylene fumarate, polyanhydrides, polyvinyl alcohol, and synthetic proteins are frequently utilized in the creation of bio-inks for 3D printing applications and are considered one of the most widely used types of synthetic biomaterials. These substances can be utilized either independently or together with natural hydrogels to

obtain particular mechanical and biological characteristics necessary for the desired purpose [55].

Synthetic polymer-based biomaterials have several advantages as bioinks for bioprinting, including their precise deposition with high fidelity and mechanical strength. Different 3D printing techniques, including extrusion-based, inkjet, and stereolithography, can be employed to accurately and carefully deposit biomaterials in a controlled fashion [80]. However, the poor biocompatibility and uncontrollable degradation of synthetic polymers remain major challenges in the development of synthetic-based bioinks [81]. Biocompatibility refers to the ability of a material to interact with biological systems without causing adverse effects such as inflammation, immune response, or toxicity. Synthetic polymers can cause adverse effects due to their chemical composition, and it is crucial to modify their surface chemistry to enhance biocompatibility. Surface modifications such as the grafting of bioactive molecules, incorporation of cell-binding domains, or functionalization with biomolecules can improve biocompatibility. Additionally, uncontrollable degradation of synthetic polymer-based biomaterials can lead to the release of toxic degradation products, affecting cell viability and function. The design of biodegradable polymers with controlled degradation rates and non-toxic degradation products is crucial to avoid these issues [82].

In summary, synthetic polymer-based biomaterials offer several advantages for bioprinting, but improving their biocompatibility and controlling their degradation remains a challenging area of research. To address these challenges, researchers have explored various approaches, including modifying the surface chemistry of synthetic polymers to enhance their biocompatibility, incorporating biologically active molecules to promote cell adhesion and growth, and developing new polymers with improved degradation profiles. As a result of ongoing research, the properties of bio-inks have been enhanced, making them more compatible with biological systems and increasing their ability to break down over time. These improvements have expanded their potential applications, which include but are not limited to tissue engineering, regenerative medicine, and targeted drug delivery [34, 83, 84].

1.5. Alginate (Alg)

Alginate is a versatile and valuable material for hydrogel-based applications in tissue engineering and drug delivery applications due to its unique properties and ease of use [85–87]. Alginate, known as derived from brown algae, is a natural polysaccharide [77]. The polymeric backbone of alginate is made up of repeating units of two different types of monomers: guluronic acid and mannuronic acid. These monomers are negatively charged, which means that alginate has an overall negative charge. Thanks to the backbone being negatively charged, alginate has the remarkable property of being able to create ionically crosslinked chains via interacting with a solution that has a positive charge, such as calcium, barium, and strontium [73, 77]. When alginate comes into contact with a solution containing ions with a positive charge, these ions bind to the negatively charged carboxylate groups on the polymer's backbone. This binding results in the formation of a structure that resembles a gel. This ionic crosslinking of alginate is widely used in biomedical applications, such as drug delivery, tissue engineering, and wound healing, due to its biocompatibility and easy processing.

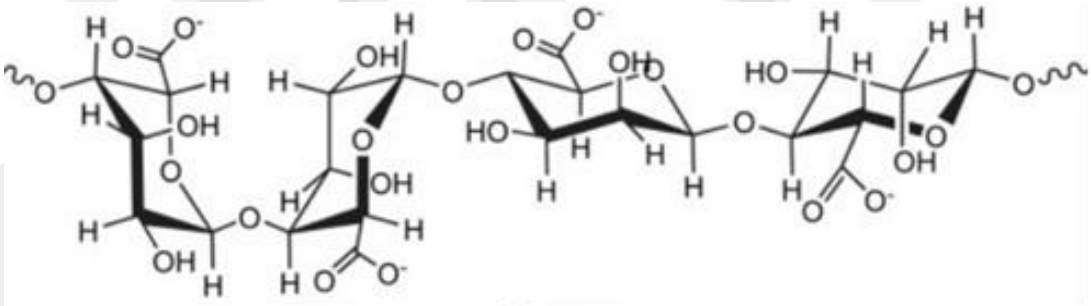

Figure 1.7 Chemical structure of alginate polymer.

One interesting property of alginate hydrogels is their pH responsiveness [88]. Alginate hydrogels are stable in a neutral to basic environment, but they can become soluble in acidic conditions due to the protonation of the carboxylic acid groups in the alginate molecule. This property makes alginate hydrogels useful for drug delivery applications, as they can release drugs in response to changes in pH. Additionally, among other things, adjusting the concentration of the crosslinking ion and the pH of the solution can control the degree of crosslinking in alginate gels. The resulting gels can have different properties, such as stiffness, porosity, and degradation rate, depending on the specific application requirements [89].

Calcium chloride ($CaCl_2$) is often used as a crosslinker for alginate hydrogel formation due to its high solubility in water, which allows for rapid ion exchange and gelation [77]. The resulting hydrogel has good mechanical strength and stability. Alginate can be crosslinked using calcium sulfate ($CaSO_4$) and calcium carbonate ($CaCO_3$) for its gelation as well [6]. However, since the water solubility of calcium sulphate ($CaSO_4$) and calcium carbonate ($CaCO_3$) is lower than that of $CaCl_2$, the time required for crosslinking also increases. This slower gelation rate can be beneficial in some cases where a slower gelation rate is desired. In addition, the choice of crosslinker can affect the properties of the resulting hydrogel. For example, the use of $CaSO_4$ as a crosslinker can result in a hydrogel with a higher porosity compared to $CaCl_2$-crosslinked hydrogels, while $CaCO_3$-crosslinked hydrogels tend to be more brittle [90].

Alginate hydrogels have been used to create various tissue constructs, such as bone, cartilage, and liver. Alginate-based hydrogels have been utilized as a means of drug delivery, with the ability to regulate the release of various bioactive molecules such as proteins and drugs. Alginate-based materials have also been utilized as wound dressings, creating a moist environment that helps facilitate the healing process.

Although alginate-based hydrogels possess several desirable characteristics for biomedical uses, such as biocompatibility and minimal toxicity, they also have certain drawbacks [91]. One such limitation is their tendency to break down over time under physiological conditions, which can limit their long-term stability. Another limitation is that alginate hydrogels do not provide binding sites for cell attachment, which can hinder cellular growth and function. One way to overcome this limitation is to incorporate cell-adhesive peptides, such as the RGD peptide, into the hydrogel [92]. These peptides can provide binding sites for cell attachment and promote cellular proliferation and function.

Besides these, alginate's ability to form hydrogels under mild conditions makes it ideal for creating bio-inks [77]. Bio-inks are essential in 3D bioprinting, a technique used to fabricate complex structures, such as tissues and organs. Alginate-based bio-inks have several advantages, such as excellent printability, high stability, and the capacity to enclose cells, growth factors, and medications [93]. The degree of

crosslinking and the concentration of the alginate solution are just a couple of the variables that can affect alginate's printability [94–97].

One way to adjust the printability of alginate is by pre-treating it with a specific amount of calcium ions before the printing process. This process, known as pre-crosslinking, refers to the addition of a small quantity of calcium ions to the alginate solution, resulting in partial crosslinking of the alginate chains. This can improve the mechanical stability of the printed structure and prevent deformation during printing.

Another way to adjust the printability of alginate is by altering the quantity and nature of the crosslinking agent used. Different crosslinking materials have different properties, such as their strength and stiffness, which can affect the final printed object. For example, adding a higher concentration of calcium ions can lead to stronger crosslinking and a more rigid structure. Alternatively, using different types of crosslinking agents, such as polyethylene glycol (PEG), can also affect the printability of alginate. Briefly, it is possible to adjust and optimize the properties of the printed object by modifying the quantity and nature of the crosslinking agent used [96].

Lastly, printing the alginate solution directly into a calcium chloride solution can also lead to quick setting and improved printability [88]. This method, known as in-situ crosslinking, involves using a bath of calcium chloride solution to crosslink the alginate as it is being printed. This can lead to more precise printing and better control over the final structure.

Zhang and colleagues used alginate-based bioinks to print cartilaginous cell hollow structures, taking advantage of these properties [98]. In this study, these container-like printable microfluidic channels gained the ability the transport essential substances like oxygen and nutrients through their structure. Additionally, the channels were found to support cell growth. Also, to develop tubular structures with a triaxial nozzle assembly, Yu and colleagues used cartilage cells and alginate as bioinks in a similar study [99]. Their findings demonstrated that the coaxial system using this particular bioink has the ability to enhance the survival of cartilage progenitor cells both during the printing process and after it, during the post-press stage. Gao and colleagues developed a coaxial system that can produce robust structures with tiny channels for delivering nutrients using a hydrogel material based

on alginate through 3D printing [100]. Likewise, Jia and co-workers described a mixed bio-ink system based on alginate that can be employed for direct 3D printing of structures [101]. Christensen and colleagues produced a bio-ink containing mouse fibroblast cells using sodium alginate and utilized a calcium chloride crosslinker in a personalized 3D printer to develop vascular-like structures [102]. Ning and co-workers employed biomaterials based on alginate to produce 3D structures that contained living cells. They examined how the flow characteristics influenced various cell lines, including Schwann cells, fibroblast cells, and skeletal muscle cells, during the printing process [103]. They also noted that the concentration of bio-ink, temperature, and viable cell density had an impact on the flow rate of cell suspensions. Additionally, in the initial printing of induced pluripotent stem cells and human embryonic stem cells, alginate was utilized as a bioink [104]. Moreover, they investigated the ability of such cells to differentiate into cells that resemble hepatocytes. Zhao and co-workers utilized 3D bioprinting to generate a tissue model of a cervical tumour and examine its in vitro characteristics [105]. To conduct their research, they employed a combination of HeLa cells and a bio-ink made up of gelatine, alginate, and fibrinogen for printing. Ahlfeld and colleagues blended synthetic nanosilicate clay with alginate and carboxymethyl cellulose (CMC), resulting in two bio-ink formulations. They evaluated the bio-ink samples using a 3D drawing technique based on extrusion to create 3D structures [106]. This approach offered high printing precision and smoother extrusion. In another study, Kosik-Kozioł and co-workers described the development of cartilage structures using 3D printing technology, made of alginate and reinforced with PLA fibers [107]. According to their results, incorporating PLA fibers into the 3D structures enhanced their mechanical properties by a factor of three when compared to structures made solely of alginate. Furthermore, the fiber-reinforced alginate constructs maintained the rounded shape of human chondrocyte cells for up to two weeks during in vitro testing. These studies provide evidence that alginate-based bioink is a highly preffered material in 3D bioprinting due to its many advantages over other hydrogels [65].

1.6. Purpose of The Thesis

According to the studies in the literature, alginate has advantages as a bioink, but it may not maintain long-term stability under physiological conditions due to ionic

cross-linking. This limits the application of ionic cross-linked alginate hydrogels in biomedical materials. In addition, it is necessary to obtain combined systems with additional components, such as RGD, to achieve this with alginates that do not have a sufficient stimulating effect on cell attachment. It is seen that combinations of alginate hydrogels with other polymers are used or different cross-linking approaches are applied, especially to increase mechanical strength. One of the methods used is photo-crosslinking, which makes alginate hydrogels with much better mechanical properties and structural stability than calcium ionic cross-linked alginate hydrogels [108, 109].

Photocross-linking is a powerful technique for in situ gelation that can create a 3D network of covalent bonds within a hydrogel using light [77]. This technique has several advantages over traditional chemical cross-linking methods, including its mild reaction conditions, the ability to cross-link in the presence of biological molecules, and the ability to create highly defined and tunable networks [110]. In photo-crosslinked hydrogel applications, cells or aqueous macromer solutions with bioactive factors can be moved in a way that is minimally invasive. After a short exposure to ultraviolet (UV) light, the solutions quickly cross-link in place under physiological conditions. For this reason, photo-crosslinked hydrogels have recently received increasing attention in biomedical applications [111, 112]. Photo-crosslinked hydrogels are made by exposing a solution with photoinitiators to UV or visible light. When exposed to UV or visible light, chemicals called photoinitiators release free radicals that can start the polymerization process. In this way, the free radicals formed convert aqueous macromer solutions into hydrogels [113, 114]. In addition, the mechanical properties and swelling behaviour of photocrosslinked hydrogels can be easily controlled by replacing the photocurable part [110, 115]. However, the speed and consistency of crosslinking, which depend on the depth of light penetration and dispersion, are significantly affected by the concentration of the initiator [116]. Some of the chemical photoinitiators used in these studies are VA-086, VA-044, V-50, and Irgacure 1870. In photoinitiator crosslinking processes, photoinitiator active groups like methacrylate (MA) are added to macromolecular chains to lower the photoinitiator concentration and keep the right amount of crosslinking [117, 118]. This protects cells and bioactive substances from damage while keeping the right amount of crosslinking. There are different alternatives for the methacrylate process.

One of them is the modification of alginate with methacrylate anhydride. Another approach is to methacrylate alginate by adding amino ethyl methacrylate (AEMA) to the structure with the help of EDC-NHS. Both methods are applied in the literature. In my thesis work, it is aimed to obtain alginate, which is the most widely used biomaterial, in a form that can be crosslinked with light in order to improve its mechanical properties and increase its integration with biological tissue.

Microwave heating is based on the fact that the material to which this energy is applied absorbs microwave energy and converts electromagnetic energy into heat. When microwave energy is applied, molecules with dipole moments absorb this energy easily, the rotational movements of the molecules are stimulated, and many chemical reactions, including polymerization, can take place at lower temperatures than normal and in short periods of time [119–121]. Since the efficiency of chemical modifications will increase as a result of microwave heating, it is expected that this method applied in our study will reduce the very long purification time due to the low methacrylation efficiency obtained with the conventional method, and also reduce the reaction time from 24 hours to minutes.

Tannic acid (TA) is a polyphenolic compound obtained from plants and is commonly employed in the design of biomaterials, including surface modification, protein alteration, and crosslinking [122]. However, according to studies, TA has valuable properties such as biocompatibility [123], antioxidant, antibacterial, and biodegradability [124, 125]. The United States Food and Drug Administration (FDA) has given TA approval and it has the capacity to interact with biopolymers like albumin, chitosan, collagen, and gelatin through non-covalent interactions [126], [127]. Previous studies have shown that TA can form cross-linked macromolecules with hydrogen, covalent, and hydrophobic bonds because it contains more than one phenolic group [128, 129]. In addition, it has been determined that the contact of TA with human tissue has adhesion, hemostasis, and antimicrobial effects [129, 130]. These properties have made TA a suitable biomaterial to form multifunctional hydrogels for use in biomedical applications, and in light of these, the spread of tannic acid applications in materials science has recently increased rapidly [122, 131, 132]. In this context, the use of TA in the work of my thesis is expected to increase antimicrobiality, and, more importantly, adhesion ability, which is reported to be low in alginate-based hydrogels [9].

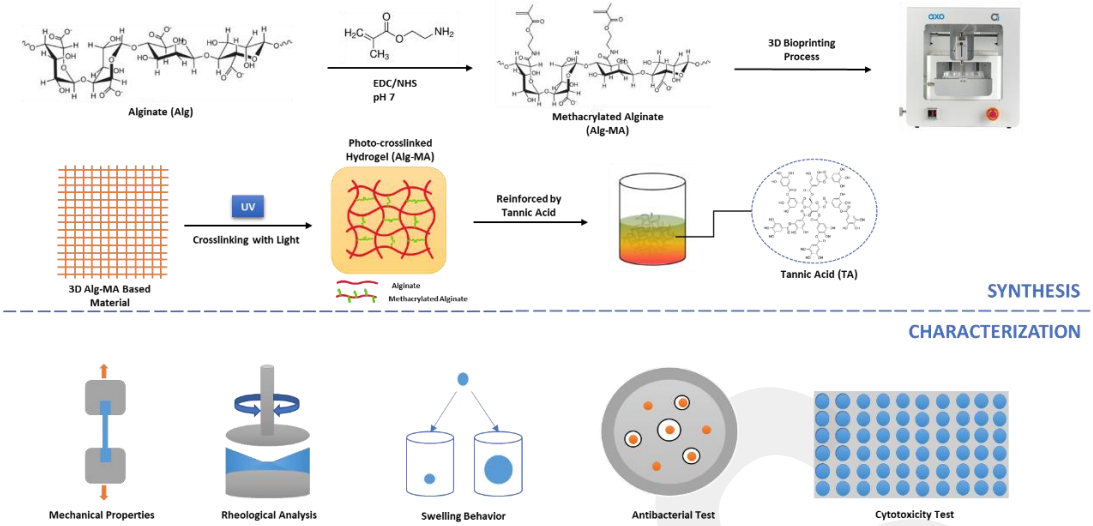

Figure 1.8 Schematic illustration of alginate-based hydrogel synthesis and characterization within the scope of this study.

When the literature is examined, although many different alginate-based bio-inks are used in three-dimensional bioprinting applications in tissue engineering, there is no photo-crosslinked alginate prepared with microwave energy with high efficiency, and there is no bio-ink application in which alginate and tannic acid materials are used together. Accordingly, in this study, we primarily aimed to improve the mechanical properties and tissue integration of alginate by increasing the reaction efficiency in crosslinking with photo-crosslinking, as well as to strengthen the weak mechanical properties of alginate by adding tannic acid to the alginate bio-ink, as well as improve the antibacterial properties of tannic acid. We aim to produce an alginate-based bioink that can be used appropriately without creating toxic effects for tissue engineering applications (Figure 1.8).

Chapter 2

2.Materials And Methods

2.1. Materials

Alginate (Alg, 180947), 2-aminoethyl methacrylate hydrochloride (AEMA, 516155), N-(3-dimethylaminopropyl)-N'-ethylcarbodiimide hydrochloride (EDC, E7750), N-Hydroxysuccinimide (NHS, 130672), lithium phenyl-2,4,6-trimethylbenzoylphosphinate (LAP, 900889), phosphate buffered saline (PBS, P4417), and tannic acid (TA, 403040) were purchased from Sigma-Aldrich (Germany). Empty 3 ml cartridge syringes (CONS-C-001) and 0.25 mm diameter bioprinting needles (CONS-BN-25G) were obtained from Axolotl Biosystems (Istanbul, Turkey).

2.2. Synthesis of methacrylated alginate (Alg-MA)

Methacrylated alginate is produced by reacting 2-aminoethyl methacrylate (AEMA) with sodium alginate (Alg) according to the method given in the literature [108]. Briefly, sodium alginate was dissolved in autoclaved filtered ultrapure (AFU) water (1% w/v, pH 7). 1-ethyl-3-(3-dimethyl aminopropyl)-carbodiimide hydrochloride (EDC) and N-hydroxysuccinimide (NHS) were then added to the alginate solution in order to activate the alginate's carboxylic acid groups (Figure 2.1). After 15 minutes, pre-dissolved AEMA (EDC:NHS:AEMA: 2:1:1, molar ratio) was added to the product, and the reaction proceeded for 24 hours at room temperature. Then, Alg-MA was purified by dialysis against distilled water for 3 days (MWCO 12-14 kDa), and lyophilized. Methacrylation was performed with conventional synthesis and also microwave irradiation in order to investigate the effect of microwave energy on the synthesis. Microwave irradiation was carried out with a temperature- and power-controlled microwave synthesis device (MicroSynth Milestone flexiWAVE).

Unlike the traditional method, in this experiment, the solution was mixed in a magnetic stirrer for 15 minutes after the pre-dissolved AEMA was added to the system. Then, the solution was transferred to the microwave device, and microwave energy was applied for 5 minutes at varying periods and microwave powers (100W, 250W, and 600W) (Table 2.1). The temperature of the synthesis reaction was kept between 50-60 ^{o}C. The microwave energy was stopped at certain intervals, and the solution was cooled with specific cycles. After synthesis was completed, the solution was purified for 3 days using 12-14 kDa dialysis tubes against distilled water and then freeze-dried. The products were characterized by ^{1}H-NMR and FTIR, and the methacrylation degree was calculated.

Table 2.1 Synthesis parameters of the Alg-MA hydrogels.

Method type	EDC (mg)	NHS (mg)	AEMA (mg)	Power (W)	Reaction Time	Dialysis Time (Day)
Conventional	95.85	28.75	41.40	-	24 hours	3
Microwave	95.85	28.75	41.40	100	6 min (40 s x 6 + 60 s x 2)	3
Microwave	95.85	28.75	41.40	250	6 min (20 s x 10 + 30 s x 5)	3
Microwave	95.85	28.75	41.40	600	6 min (10 s x 20 + 20 s x 8)	3

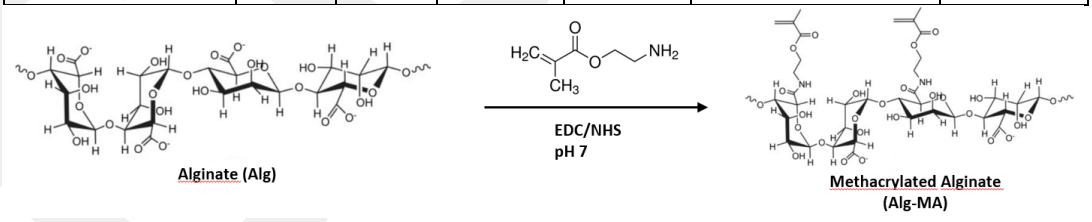

Figure 2.1 Methacrylation reaction of alginate.

2.3. Preparation of photo-crosslinked Alg-MA hydrogels

To fabricate photo-crosslinked Alg-MA hydrogels, Alg-MA (1%, w/v) was dissolved in AFU water containing 0.3% w/v photo-initiator (LAP). Alg-MA

solutions were injected into glass plates and crosslinked with 365 nm UV light at 3000 mW/cm2 (Woodpecker B-Cure Plus) for 30 seconds to make hydrogels with a diameter of 10 mm and a height of 10 mm (Figure 2.2).

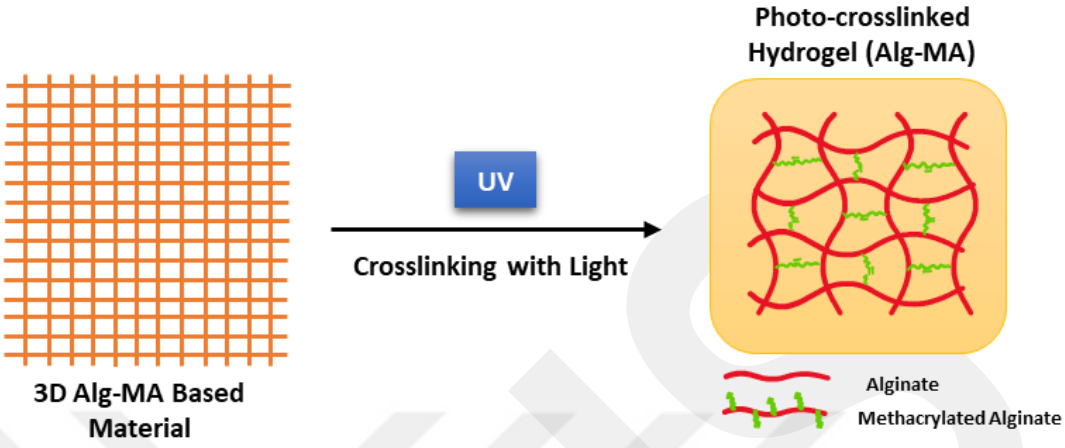

Figure 2.2 Illustration of Alg-MA hydrogels after photocrosslinking.

2.4. 3D Printing

The 3D printing of Alg-MA samples was performed with a 3D printer (Axo A1 brand). First, Alg-MA (3% w/v) solution containing 0.3% LAP was prepared with AFU water. A preliminary crosslinking was applied by mixing the prepared solution with 1% $CaSO_4$ (2:1, v/v). Then, the hydrogel solution was transferred to the syringes and centrifuged at 1500 rpm for 5 min to remove the bubbles (Figure 2.3) [133]. The printing process was carried out at room temperature using a 25G nozzle.

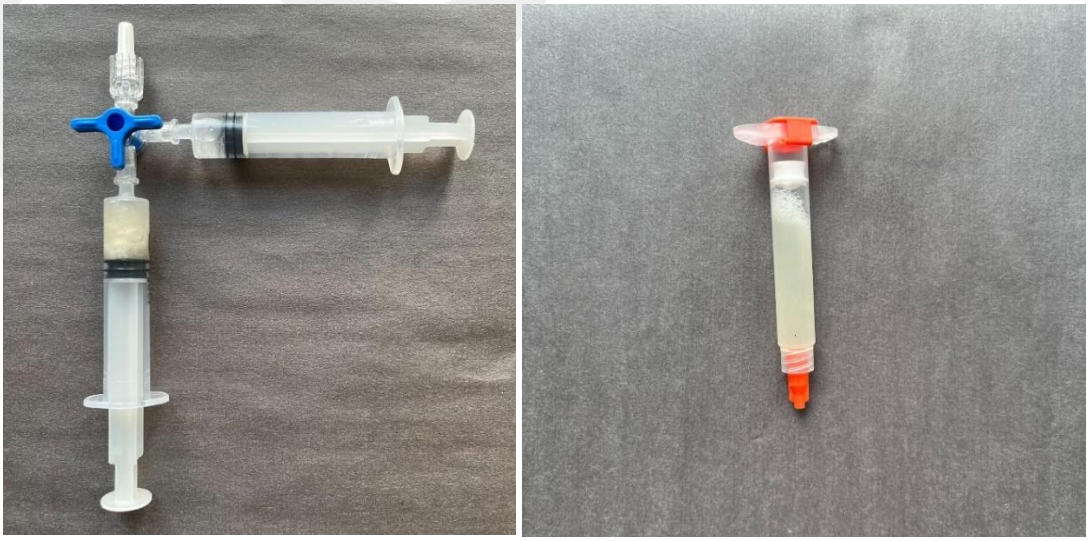

Figure 2.3 Images of alginate hydrogels in the syringes prepared for the printing process.

For the printing study, the resolution of the printed Alg-MA filaments was evaluated in two dimensions: width and height. For this purpose, different pressures (4, 5, 6, 7, and 8 psi) and speeds (5, 10, 15, 20, and 25 mm/s) were applied. Alg-MA filaments were exposed to UV for 30 s after printing, and then images were taken. The width and height measurements of the images were noted using ImageJ software. These values were then plotted with the GraphPad software.

2.5. Preparation of Tannic Acid (TA) loaded hydrogels

Photocrosslinked Alg-MA hydrogels were exposed to various amounts of TA solution [124, 125, 134]. Briefly, three different concentrations of TA (0.5%, 2.5%, and 5%, w/v) were prepared, and photo-crosslinked Alg-MA hydrogels were immersed into these solutions for 24 h at R.T (Figure 2.4). Then, the hydrogels were rinsed with distilled water and lyophilized. Hydrogels were characterized by FTIR to prove the addition of TA into the structure by observing broad bands from 3000 to 3550 cm-1, and peaks at 1713 cm-1 and 1613 cm-1. The antibacterial effect of TA at different concentrations on the hydrogels was evaluated by gram-positive (Staphylococcus aureus) and gram-negative (Escherichia Coli) bacteria. The stability, swelling, and mechanical characterization of the hydrogels were evaluated.

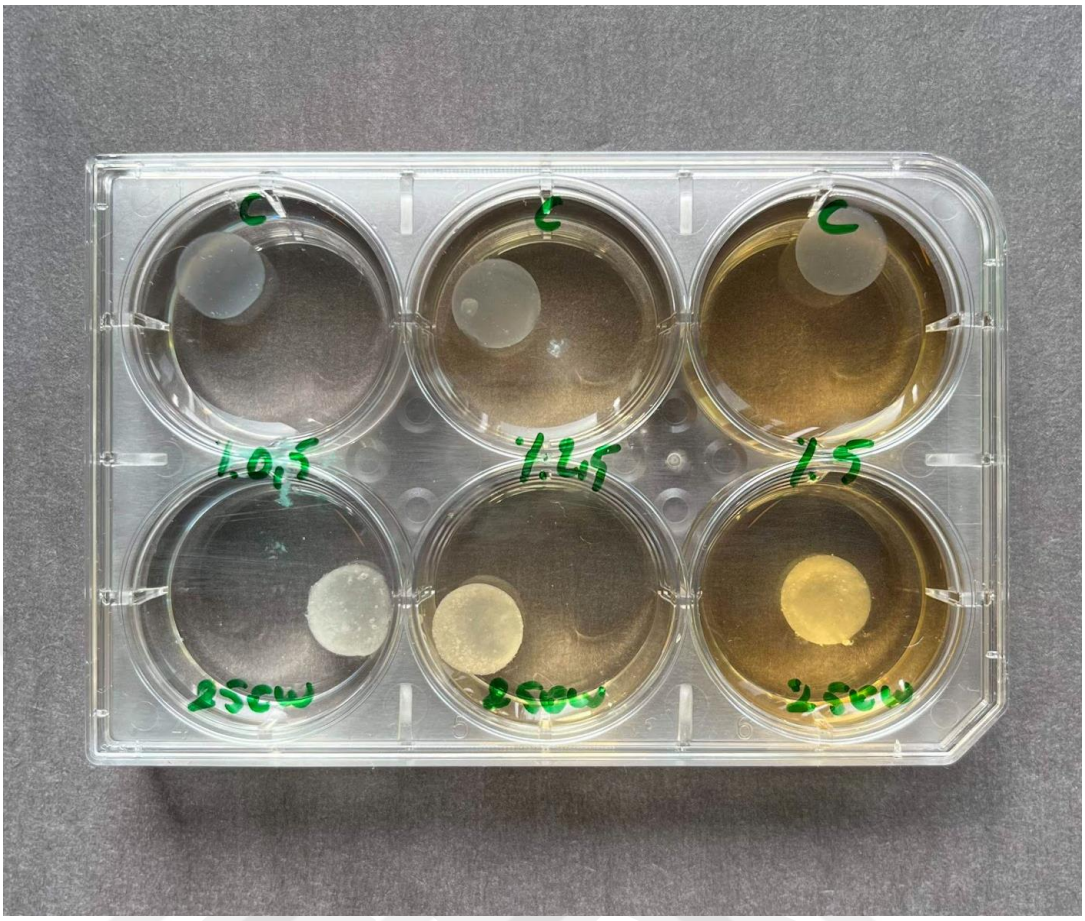

Figure 2.4 Tannic acid-immersed hydrogels.

2.6. Characterizations

2.6.1. ^{1}H-NMR Characterization

The ^{1}H-NMR analysis for all samples was performed by a Bruker 400 brand/model (400 MHz) device, and the degree of methacrylation (DM) for all Alg-MA samples was determined from ^{1}H-NMR spectra. All samples containing Alg-MA were dissolved to a concentration of 1% (w/v) in deuterium oxide (D_2O). Unmodified alginate was used as a reference. The percent DM (DM%) on the Alg backbone was calculated utilizing the equation below [135]:

$$DM\% = \frac{(H_a / 3) + [(H_b + H_c) / 2]}{H_{Alg} / 2} \times 100 \quad (2.1)$$

where H_{Alg} stands for protons in the Alg backbone; H_a, H_b, and H_c stand for protons in the methyl group and vinyl group of AEMA, respectively.

2.6.2. FT-IR Characterization

The FTIR analysis was performed using a Thermo Scientific Nicolet 6700 with ATR mode (4000-400 cm^{-1}) in order to evaluate the chemical structure of hydrogels, and unmodified alginate was taken as a reference. The peaks at 2980-2850 cm^{-1} (-CH streching) and 1714 cm^{-1} (COO- streching) from the methacrylate units and the peaks at 1713 cm^{-1} and 1613 cm^{-1} (COO-) from the addition of tannic acid were used for the assessment [134, 136, 137].

2.6.3. SEM Analysis

SEM analysis has been carried out using the Zeiss Gemini 300 instrument. For this analysis, all hydrogel samples were dried and then coated with gold. The coated hydrogel samples were appraised with regard to surface and cross-section morphologies.

2.6.4. Rheological Analysis

The rheological properties of the hydrogels were measured using an Anton Paar MCR 301 brand/model instrument. Hydrogels were obtained in the form of a cylindrical disk of 2 mm in height and 12 mm in diameter. Rheological properties were evaluated on three different main parameters: frequency, strain, and temperature. Frequency-dependent rheological analysis was performed under 0.2% strain between 0.5 and 100 rad/s. As a result of the dynamic analysis, the storage modulus (G'), loss modulus (G''), and complex modulus (G*) values of the hydrogels were determined. Strain-dependent rheological analysis was performed at a fixed frequency of 1 Hz, at a strain range of 0-2%. As a result of the dynamic analysis, the G', G'' and G* values of the hydrogels were determined. In order to see the structural stability of the hydrogel at different temperatures, temperature-dependent rheological analysis was carried out at a constant frequency of 1 Hz, in the range of 15-45 °C. As a result of the dynamic analysis, the shear stress of the hydrogels was determined.

In addition, a 3% w/v solution was prepared with both conventional and microwave methods (100W, 250W, and 600W) and non-methacrylate alginate samples. Then, in order to see whether the solutions were suitable for printing on a 3D bioprinter, the temperature was increased by 0.5 °C every 30 seconds, and the viscosity was determined in a rheometer (Anton Paar, Austria) in the range of 15-45 °C.

2.6.5. Mechanical Tests

The mechanical properties of the hydrogels were evaluated in the SHIMADZU AG-X 50kN brand/model universal testing instrument in order to evaluate the compressive moduli of the hydrogels. The hydrogels were acquired in the form of a cylindrical disk of 10 mm in height and 10 mm in diameter. The test was performed by applying compression force at R.T. A compression force 0.05 N was applied at a displacement rate of 0.02 mm/sec. Before the mechanical test, all samples were stored in PBS.

2.6.6. Swelling and Stability

In order to determine the swelling capacity and stability of the obtained photo-crosslinked and TA-enhanced hydrogels, the disks, which are 12 mm in diameter and 2 mm in height, were lyophilized and then submerged in PBS solution (pH 7.4) at 37 °C. Different time intervals were applied for both swelling (15, 30 min, 1, 2, 4, 6, and 8 h) and stability tests (3, 7, 14, 21 and 28 d) [138]. The PBS solution was changed every 2 days over the tests, and the tests for all samples were repeated three times. The percentages of swelling and stability were calculated by the equations (2.2 and 2.3) given below. Note that weight loss was calculated for the assessment of hydrogel stability.

$$\text{Swelling capacity (\%)} = (W - W_0) / W_0 \times 100 \quad (2.2)$$

In this equation, W is the weight of the swollen material, and W_0 is the weight of the dry material before immersing.

$$\text{Weight loss (\%)} = (W_0 - W_d) / W_0 \times 100 \quad (2.3)$$

In this equation, W_0 is the dry weight of the material before degradation, and W_d is the dry weight of the material taken from the environment at a given time.

2.6.7. Antibacterial Test

The antibacterial activity of TA-containing Alg-MA materials was determined by the Kirby-Bauer disk diffusion test. For this purpose, the bacterial species Staphylococcus aureus (S. aureus) and Escherichia coli (E. coli), representing gram-positive and gram-negative types, respectively, were cultured separately in a liquid nutrient medium called LB Broth. By measuring the OD600 values, the bacteria were brought to 0.5 McFarland density and inoculated with a sterile swab on the surface of

the petri dish containing LB agar. Then, Alg-MA/TA materials (5 mm in diameter) and an ampicillin disc as a positive control were placed in a petri dish (100 mm). The discs were incubated at a temperature of 37 ^{o}C for 24 h. The area around the discs where bacterial growth was inhibited was then measured and compared to the negative control (non-TA hydrogel) to determine the antibacterial activity.

Chapter 3

3.Results and Discussions

3.1. Determination of the degree of methacrylation (DM)

Since the degree of methacrylation has a considerable influence on the physical properties of the material, it is critical to calculating the DM using proton NMR spectra. For this reason, ^{1}H-NMR spectra of alginate, conventionally methacrylated alginate, and alginate methacrylated by microwave method using different powers were obtained for NMR analysis as shown in Figure 3.1. When the spectra were analyzed and DM was calculated according to Equation 2.1, it was observed that the methacrylating process of all samples was carried out successfully.

Figure 3.1 shows both the characteristic peaks belonging to the saccharide units of alginate and newly formed amide bonds formed by the reaction of alginate with 2-aminoethyl methacrylate (AEMA). Here, the characteristic peaks between 3.50 ppm and 5.20 ppm are observed in all spectra and represent the saccharide units of alginate [136]. In addition, the peaks at 5.76 and 6.16 ppm in the Alg-MA samples represent vinyl protons of AEMA, while the peak at 1.95 ppm represents methyl protons [108]. Furthermore, the peaks around 3.25 ppm represent the protons of the methylene group attached to the amide group.

Considering these peaks, it was observed that the methacrylation degree of Alg-MA hydrogels obtained by the microwave method was higher than that of Alg-MA hydrogels obtained by the conventional method, as shown in Table 3.1. When the microwave assisted Alg-MA samples were analyzed among themselves, it was observed that the hydrogel samples obtained by applying 250W power showed a

higher methacrylation degree compared to the others. In addition, it was also observed that a noticeable increase in temperature was obtained with the energy applied during microwave synthesis. Therefore, during the synthesis using 600W energy, the solution reached much higher temperatures than those using 100W and 250W energy. Considering this situation, the lower degree of methacrylation in the samples synthesised with 600W energy compared to the others was achieved due to the elevated temperature having an unfavorable effect on the methacrylation reaction.

Taking into account all these results, we can conclude that microwave irradiation allowed for more efficient methacrylation in shorter reaction times compared to conventional synthesis.

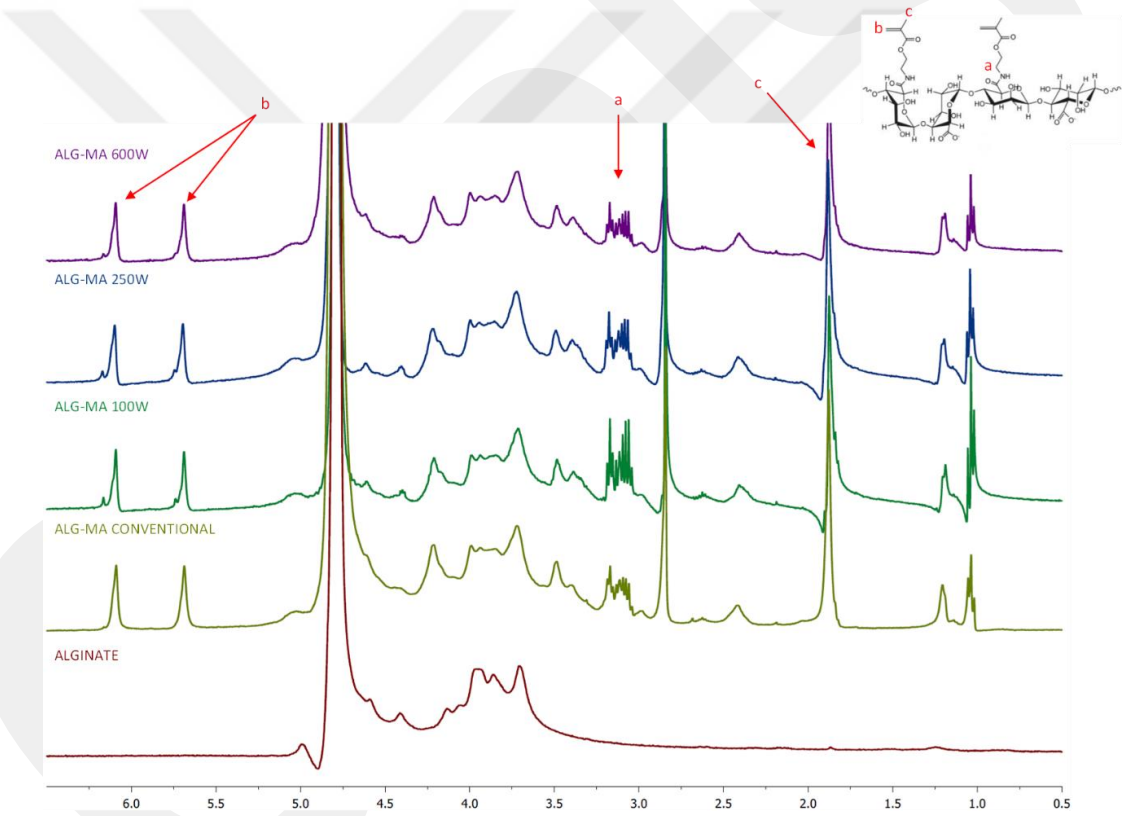

Figure 3.1 NMR spectra of methacrylated alginates (with 100, 250, and 600 W microwave irradiation) and conventional samples.

Table 3.1 Degree of methacrylation of Alg-MA samples.

Samples	Degree of methacrylation (%)
ALG-MA CONVENTIONAL	66
ALG-MA 100W	71
ALG-MA 250W	83
ALG-MA 600W	63

3.2. 3D Printing

Although we used cylindrical needles in 3D bioprinting, the printed structures do not have a cylindrical form. In addition, the printed hydrogels have certain weights, and gelation rates are slow. Therefore, these hydrogels are prone to diffusion and spreading from their initial shape [139, 140]. Due to this reason, the printing resolution of the hydrogel filaments to be printed was evaluated in two dimensions: height and width. For this, firstly, 3% (w/v) Alg-MA was mixed with 1% (w/v) $CaSO_4$ for pre-crosslinking, and then 3D printing was performed under different pressures (4, 5, 6, 7, 8 psi) and speeds (5, 10, 15, 20, 25 mm/s). The printed filaments were then cross-linked with UV, and images were taken with an optical microscope. Using the ImageJ program, the height and width values were measured, and the following graphs, as seen in Figures 3.3 and 3.4, were obtained to determine the optimum printing parameters.

Figure 3.2 Image of the Axo A1 3D bioprinter used in the study.

When the graphs were examined, it was observed that the height and width of the printed filaments decreased with decreasing pressure and increasing speed. In short, the height and width of the printed filaments are directly proportional to the pressure and inversely proportional to the speed. While interpreting the results, the inner diameter of the needle used during printing (25G, 250 μm) was taken into consideration. According to these results, when the height graph was analyzed, it was observed that bioprinting at 4 psi pressure at a speed of 5 mm/s and 6 psi pressure at a speed of 10 mm/s were estimated as appropriate. When the width graph was examined, the closest value to the needle tip was obtained at a speed of 20 mm/s and 25 mm/s at 4 psi pressure and 25 mm/s at 5 psi and 6 psi pressure, respectively.

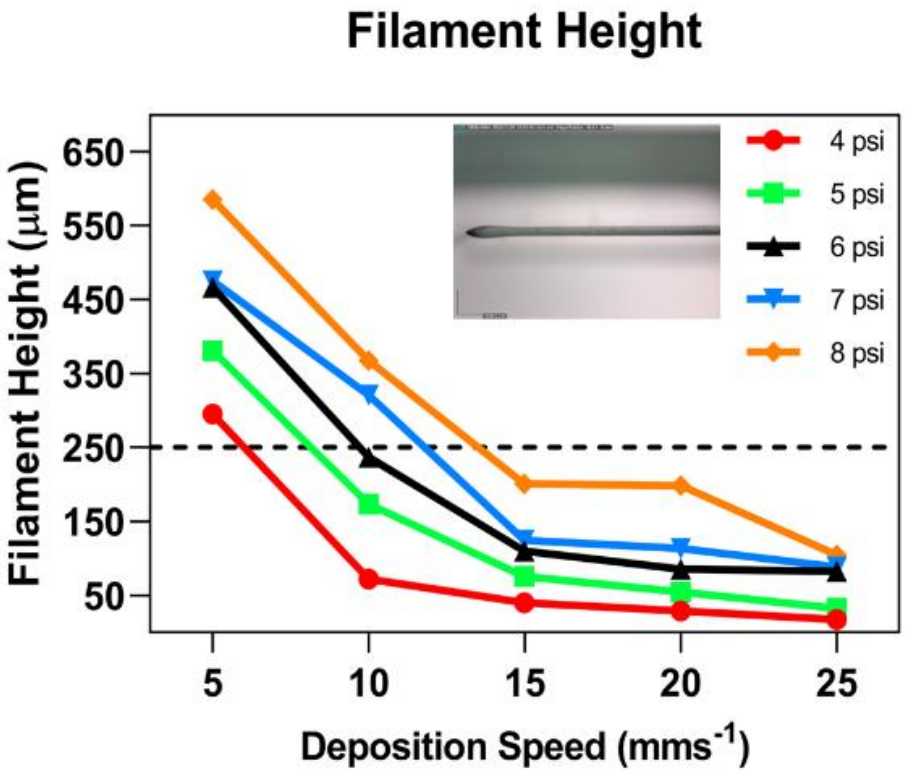

Figure 3.3 Height plot of printed hydrogel filaments.

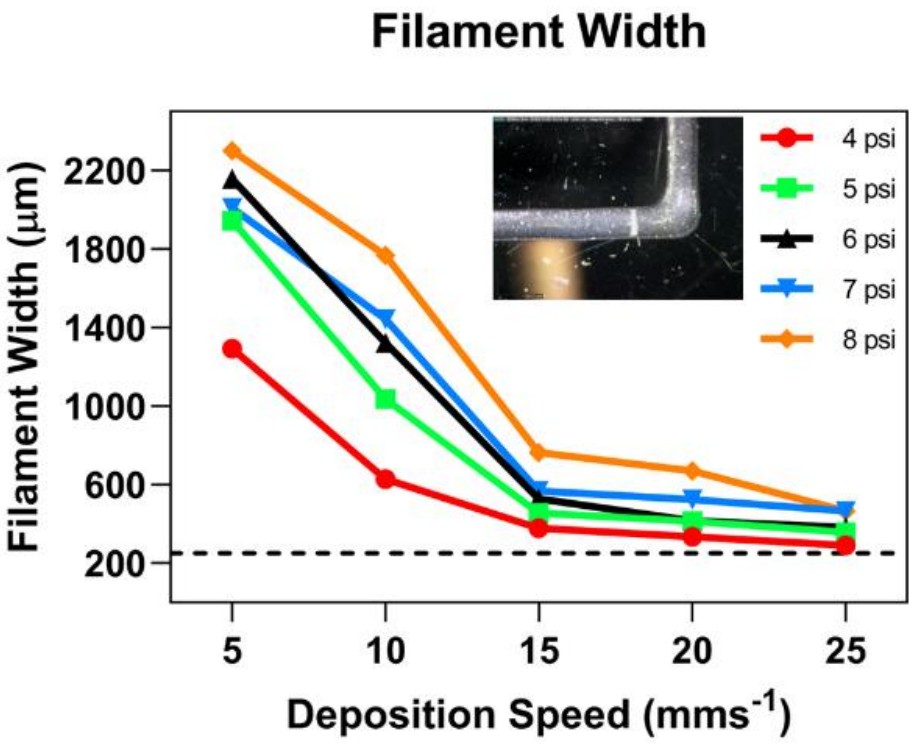

Figure 3.4 Width plot of printed hydrogel filaments.

3.3. FT-IR Analysis

In order to demonstrate the successful methacrylation of the Alg-MA samples obtained by both conventional and microwave-assisted methods and show the addition of tannic acid in varying amounts (0.5%, 2.5%, and 5% TA) into the hydrogel structure, FTIR analyses were performed and shown in Figures 3.5, 3.6, and 3.7.

When Figure 3.5 is examined, the characteristic peaks at 3700–3000 cm^{-1} correspond to the stretching in the -OH groups of alginate [136]. The peaks at 2980–2850 cm^{-1} correspond to the stretching of -CH groups [141]. In addition, when the alginate graph is analyzed, seven distinctive peaks belonging to alginate are observed. Here, the peaks at 1600 cm^{-1} and 1406 cm^{-1} correspond to asymmetric and symmetric O-C-O stretching of COO- (carboxylate anions) groups, respectively [141, 142], C-O and C-C stretching vibrations correspond to peaks at 1083 cm^{-1} and 1025 cm^{-1} respectively [141], the peak at 943 cm^{-1} corresponds to C-O stretching [141], C1-H distortion corresponds to the peak at 879 cm^{-1} [141] and finally, the peak at 817 cm^{-1} corresponds to C-H bending vibrations [143]. On the other hand, in the regions indicated by arrows, the peaks at 2980–2850 cm^{-1} of the methacrylated alginate samples show growth and a shoulder around 1715 cm^{-1}, which is not seen in the alginate spectrum. These growths and shoulders correspond to -CH groups in aliphatic chains and C=O groups in esters, respectively, as a result of the addition of methacrylate units. These results provide evidence for the successful methacrylation of alginate.

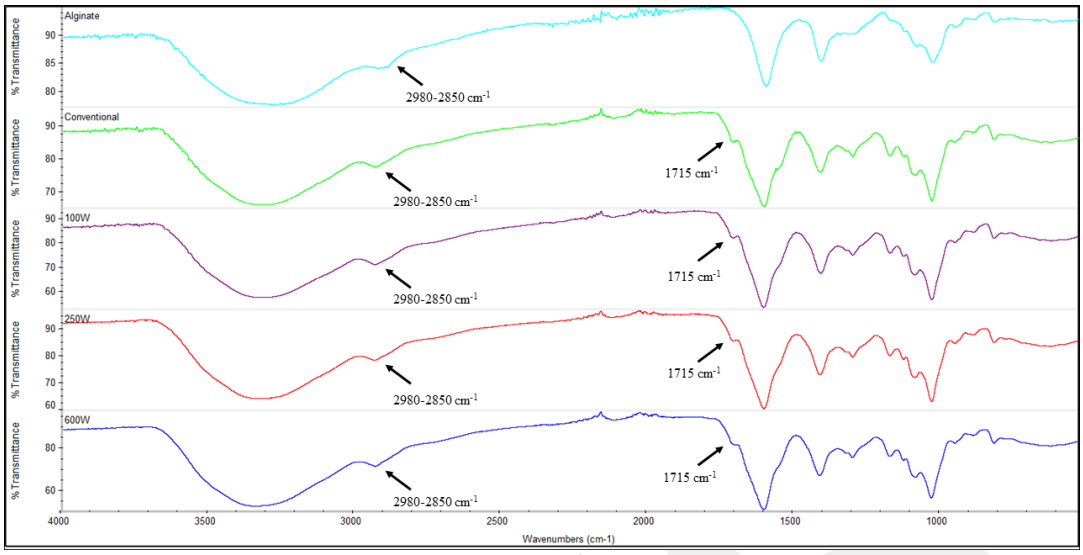

Figure 3.5 FTIR spectra of non-modified alginate and methacrylated alginates by conventional and microwave irradiation.

When Figures 3.6 and 3.7 are analyzed, a broad band between 3550-3000 cm^{-1} is observed. This band is attributed to stretching vibrations of -OH groups commonly found in phenolic groups of TA [137]. The peak at 1713 cm^{-1} corresponds to the stretching of C=O groups in ester groups [144]. The peaks at 1613 cm^{-1}, 1525 cm^{-1} and 1450 cm^{-1} can be attributed to aromatic C=C stretching [145]. Finally, the peaks at 1178–1017 cm^{-1} and 745 cm^{-1} correspond to the stretching of the benzene ring and the bending vibration of the aromatic C-H group, respectively [127]. As a result, the distinctive peaks of tannic acid are observed in the spectra of tannic acid at all

concentrations. This shows that all concentrations of tannic acid and methacrylated alginate hydrogel groups interacted successfully.

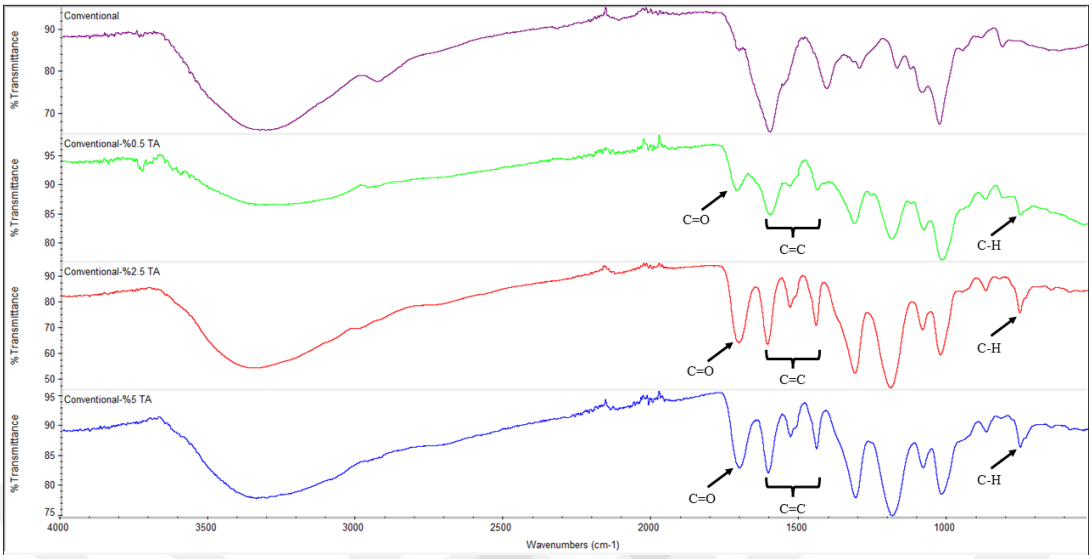

Figure 3.6 FTIR spectra of TA-reinforced hydrogels obtained by the conventional method.

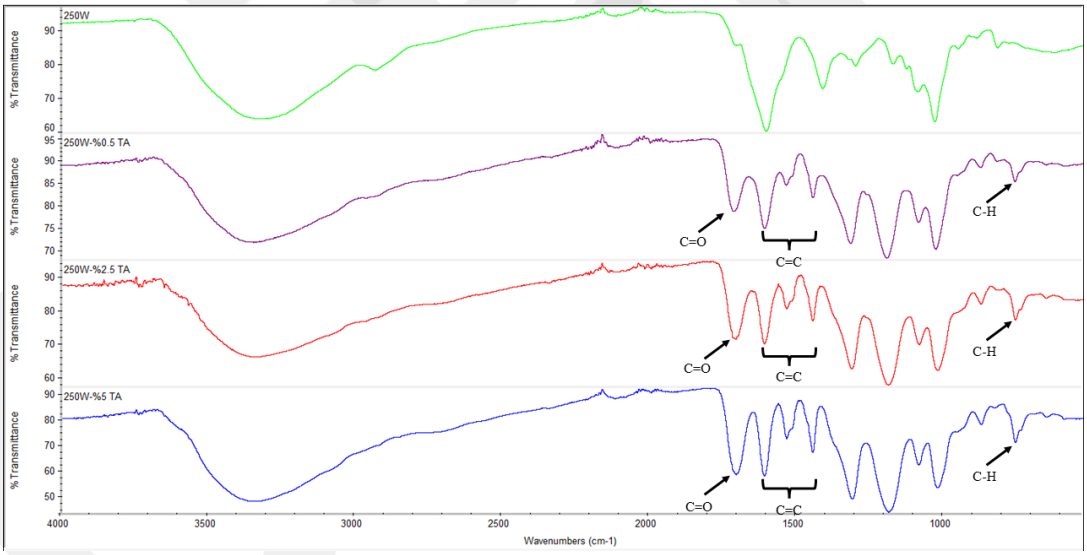

Figure 3.7 FTIR spectra of TA-reinforced hydrogels obtained by the microwave-assisted method (250 W).

3.4. Mechanical Tests

In this part of the study, 3D printed methacrylated alginate (Alg-MA) samples were UV photo-crosslinked, and the mechanical properties of the resulting Alg-MA hydrogels were investigated. Here, all Alg-MA samples (3% w/v) containing 0.3% photo-initiator (LAP) were injected into glass plates and photo-crosslinked with 365

nm UV light at 3000 mW/cm2 for 30 sec in order to the form of cylindrical disks. In addition, the photo-crosslinked hydrogels were immersed in tannic acid at varying concentrations (0.5%, 2.5%, and 5% TA) for 24 hours, and then the effect of tannic acid on the mechanical properties of the hydrogels was also investigated. Accordingly, the stress-strain curves of the hydrogels without tannic acid are shown in Figure 3.8, and the stress-strain curves of "Conventional Alg-MA" and "250W Alg-MA" hydrogels after interaction with tannic acid are shown in Figures 3.9 and 3.10, respectively. As seen in Figure 3.8, the 250W Alg-MA hydrogel with the highest methacrylation degree showed the highest resistance to deformation. A higher modulus of compression was observed with 250W irradiated hydrogels than with the conventional sample. But, a higher strain level was reached with conventional hydrogels compared to the 250W irradiated hydrogels. According to Figure 3.8, the compressive strength values for each hydrogel are 6.02, 1.93, 8.33 and 3.74 kPa for conventional, 100W, 250W, and 600W, respectively. Based on this finding, 250W irradiated samples can be used for further experiments.

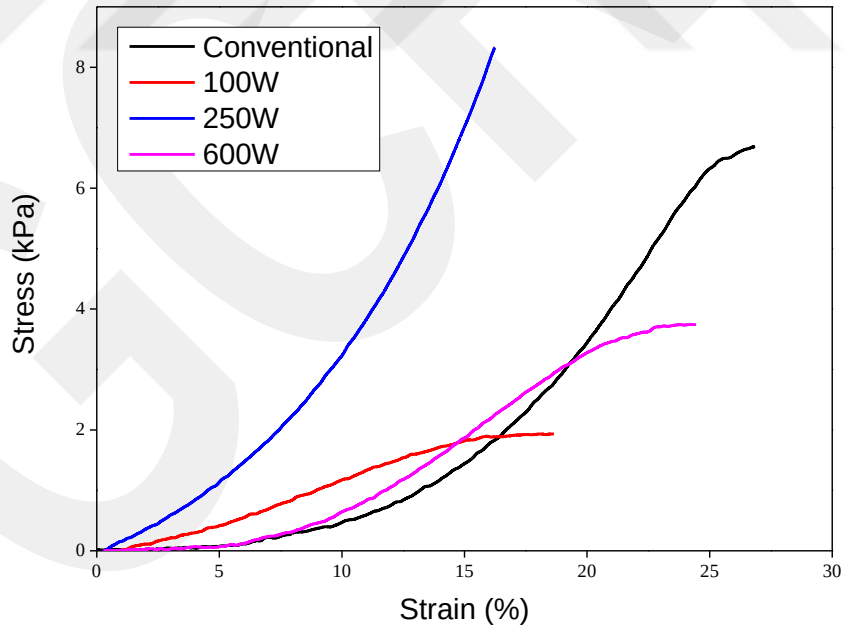

Figure 3.8 Compressive stress-strain curves of alginates.

In this study, tannic acid is used to reinforce hydrogels by adding second cross-links into the hydrogel structure. When Figures 3.9 and 3.10 were analyzed, a significant enhancement in the mechanical properties of tannic acid reinforced hydrogels was

observed compared to the hydrogels without tannic acid (non-TA). This increase in deformation resistance can be attributed to the higher crosslinking density achieved by tannic acid. For example, compressive stress was measured at 8 kPa with 15% strain, while it was 9–10 kPa with 25% strain with tannic acid reinforced hydrogels. In conclusion, it was proved that the addition of tannic acid to hydrogels synthesized by both conventional methods and microwave-assisted methods provided a significant improvement on the mechanical properties of hydrogels, as also reported in the literature [146].

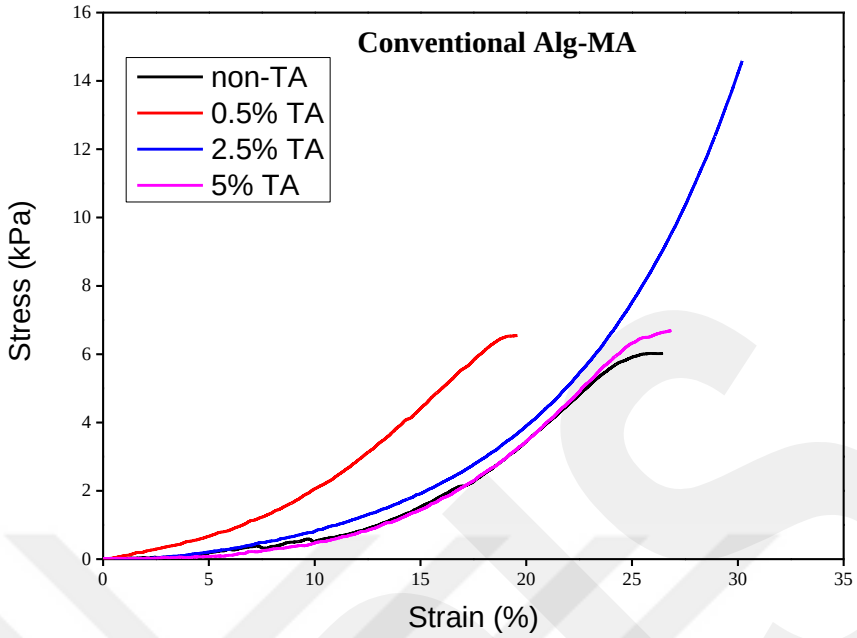

Figure 3.9 Compressive stress-strain curves of conventional Alg-MA hydrogels with different concentrations of TA.

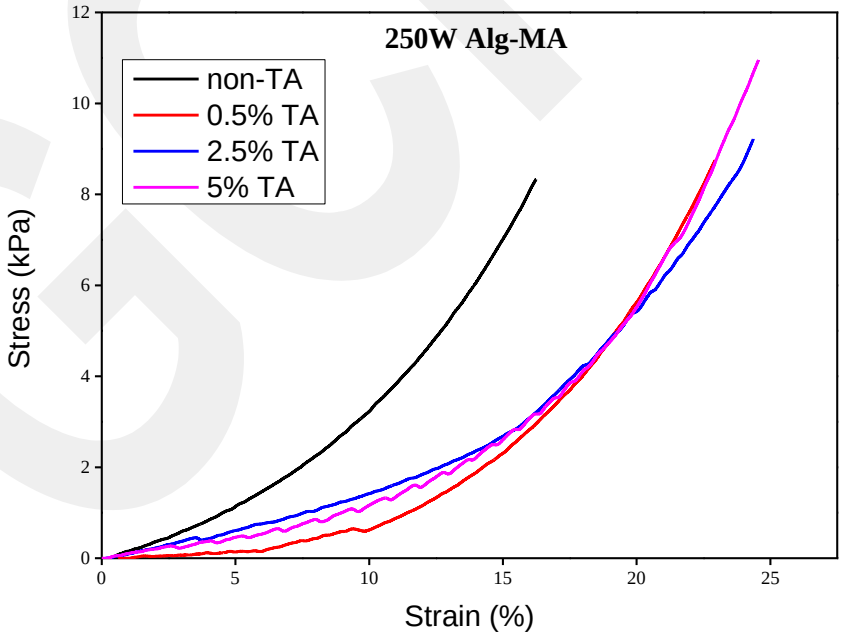

Figure 3.10 Compressive stress-strain curves of 250W Alg-MA hydrogels with different concentrations of TA.

3.5. Rheological Analysis

The rheological analysis of a bioink is a critical parameter to consider when developing a hydrogel for use in three-dimensional bioprinting, in order to maintain its shape before crosslinking. Alginate hydrogels mostly have a limited viscosity value. Bioink hydrogels with this limited viscosity tend to form collapsed structures, unable to maintain their shape [138]. Too high viscosity has a negative effect on the controlled realisation of the bioprinting, as clogging of the needle tips can occur. In addition, high viscosity will have a negative effect on cell viability in cell printing studies as it will require high pressure in extruded systems. As a result, it is very difficult to establish the ideal printing parameters needed for bioprinting without looking at the bioink's viscosity characteristics through rheological analysis [147].

In light of this information, the changes of viscosity values in methacrylated alginate hydrogels before crosslinking at a certain temperature range (15–45 ^{o}C) were investigated. Furthermore, alginate (Alg) and precross-linked alginates (Alg-$CaSO_4$) were used as controls to compare with the viscosity values of methacrylated alginate samples (Conventional Alg-MA, 100W Alg-MA, 250W Alg-MA, 600W Alg-MA). Considering Figure 3.11, it is shown that the Alg sample has the lowest viscosity value, which supports the knowledge that alginate has limited viscosity. The viscosity values of conventional Alg-MA, 100W Alg-MA, 250W Alg-MA and 600W Alg-MA vary in the ranges of 673-512 mPa.s., 1893-645 mPa.s., 2223-781 mPa.s. and 3207-631 mPa.s., respectively. According to these values, considering the Alg-$CaSO_4$ sample with known printability and viscosity values ranging between 2430-1205 mPa.s., it can be said that Alg-MA samples showed a printable bioink property for use in extruded bioprinting processes. However, the conventional Alg-MA sample showed the lowest viscosity value among the methacrylated alginate samples, with a value between 673-513 mPa.s., which proved that the Alg-MA samples produced by the microwave-assisted method provided more suitable printability in the extruded bioprinting process than the one produced by the conventional method.

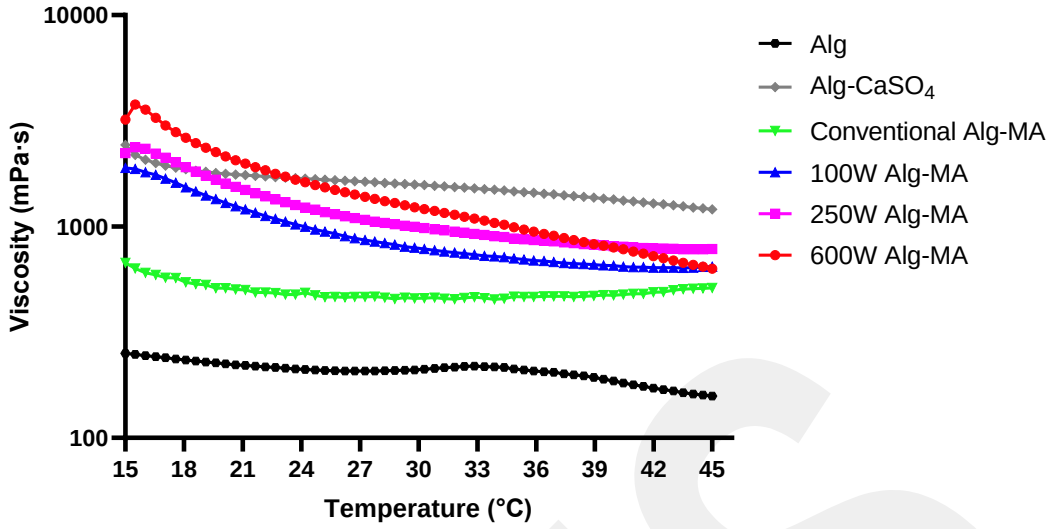

Figure 3.11 Viscosity of the alginate-based hydrogels before crosslinking.

Frequency dependent dynamic analyses, strain dependent dynamic analyses and temperature dependent shear stress of all Alg-MA hydrogels prepared with 0.3% (w/v) LAP at 3% (w/v) concentration and crosslinked by exposure to UV light for 30 seconds are shown in the Figures below (Figure 3.12, Figure 3.13, Figure 3.14, Figure 3.15, Figure 3.16). According to the frequency dependent dynamic analysis with frequency ranging from 0.5-100 rad/s, it was observed that all hydrogels exhibited elastic properties and maintained their structural integrity as shown in Figures 3.12 and 3.13. The storage modulus (G') was higher than the loss modulus (G") for all samples, which means that they showed the rheological behaviour characteristic of a gel. 100W Alg-MA and 250W Alg-MA hydrogels were found to have higher elasticity compared to the others, which can be attributed to the high degree of methacrylation showing high elasticity. It was also observed that the storage modulus (G') increased more than the loss modulus (G") with frequency in all Alg-MA groups. Accordingly, all Alg-MA groups have viscoelastic structure since G' > G".

From these frequency dependent dynamic analyses, the values of the storage modulus and Tan δ (Tan δ = G"/G') at 1 Hz were calculated. These modulus are in the range of those reported in the literature for alginate–cellulose inks that report values from the order of hundreds of Pa [148] to the order of several kilopascals [149, 150]. In our study, Tan δ values was found as 0.022, 0.039, 0.033, and 0.017 for

conventional Alg-MA, 100W Alg-MA, 250W Alg-MA, and 600W Alg-MA hydrogels, respectively.

As can be seen in Figures 3.14 and 3.15, according to the strain dependent dynamic analysis applied in the range of 0-2%, it was observed that deformation started between 0.02% and 0.03% for all hydrogels. However, considering the storage modulus, 100W Alg-MA and 250W Alg-MA hydrogels showed higher deformation resistance than the others. Conventional Alg-MA hydrogel showed the lowest deformation resistance and the lowest stable behaviour, which is an indication that more deformation resistant hydrogels can be obtained by microwave assisted synthesis compared to the conventional method. Finally, when Figure 3.16 is examined, according to the temperature dependent shear stress between 15-45 ^{o}C, Conventional Alg-MA hydrogel showed the highest shear stress while 100W Alg-MA hydrogel showed the lowest shear stress. The 250W Alg-MA hydrogel showed a slow increase in shear stress up to about 30 ^{o}C, while it showed a sharp increase after 30 ^{o}C. The 600W Alg-MA hydrogel showed a very slight increase up to 17 ^{o}C and a constant shear stress after 17 ^{o}C. According to the temperature dependent shear stress results, it is understood that 250W Alg-MA and Conventional Alg-MA will show a

more stable structure and a higher mechanical strength compared to the others, especially considering the values at 37 ^{o}C, which is the normal body temperature.

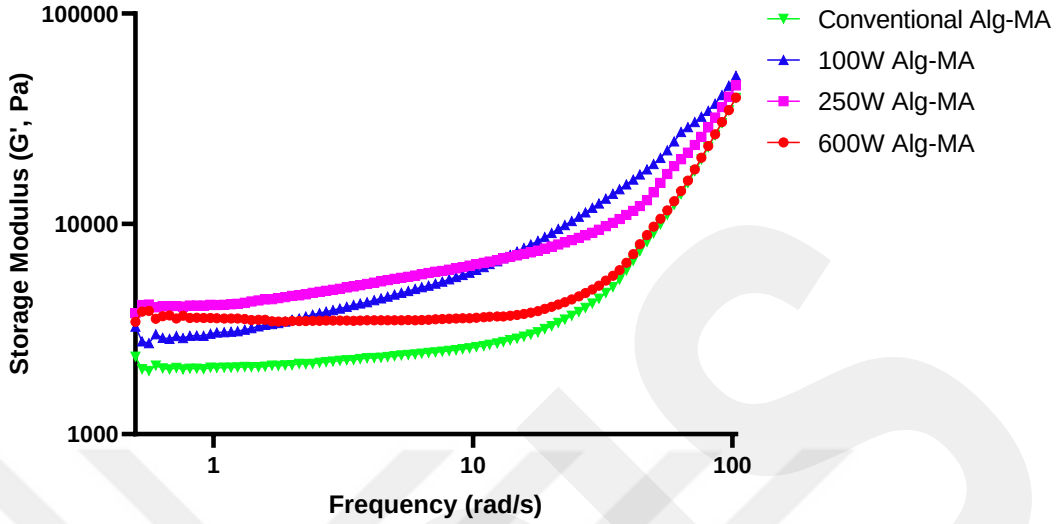

Figure 3.12 Frequency-dependent storage modulus of Alg-MA hydrogels after crosslinking.

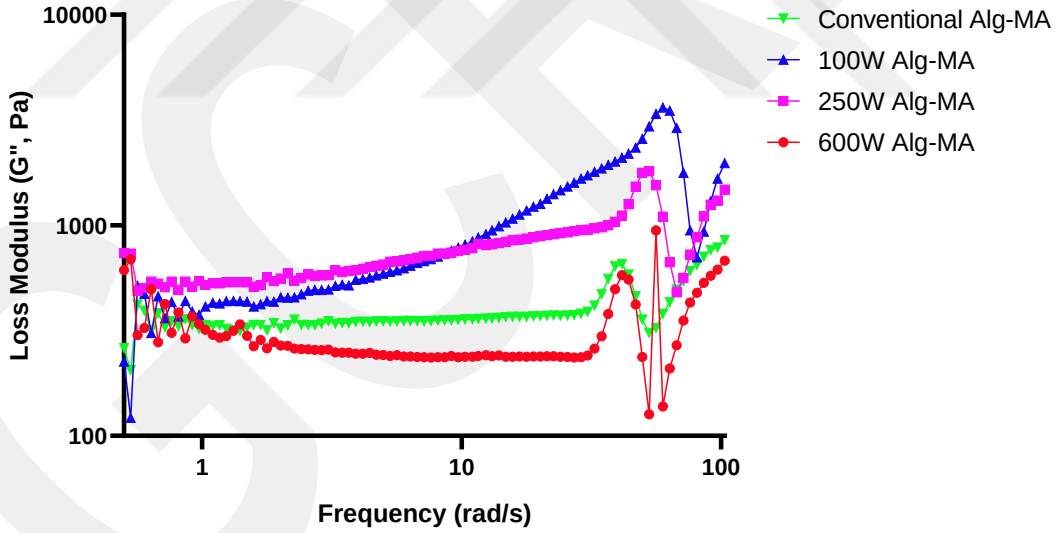

Figure 3.13 Frequency-dependent loss modulus of Alg-MA hydrogels after crosslinking.

Table 3.2 Characteristics of Alg-MA hydrogels at 200 rad/s frequency.

Samples	Storage Modulus (G', kPa)	Loss Modulus (G", kPa)
Conventional Alg-MA	39,7	0,9
100W Alg-MA	50,6	1,9
250W Alg-MA	45,5	1,5
600W Alg-MA	39,9	0,7

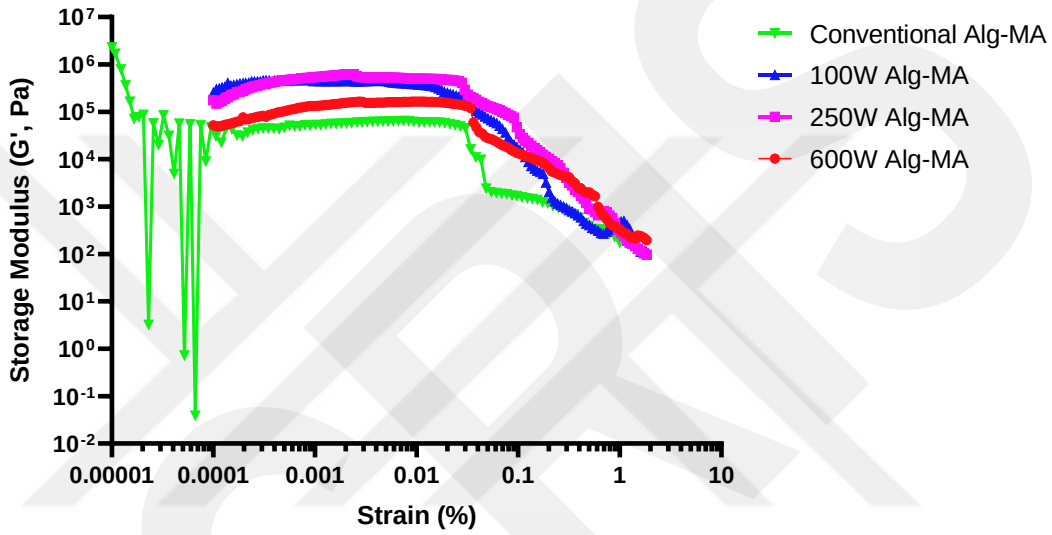

Figure 3.14 Strain-dependent storage modulus of Alg-MA hydrogels after crosslinking.

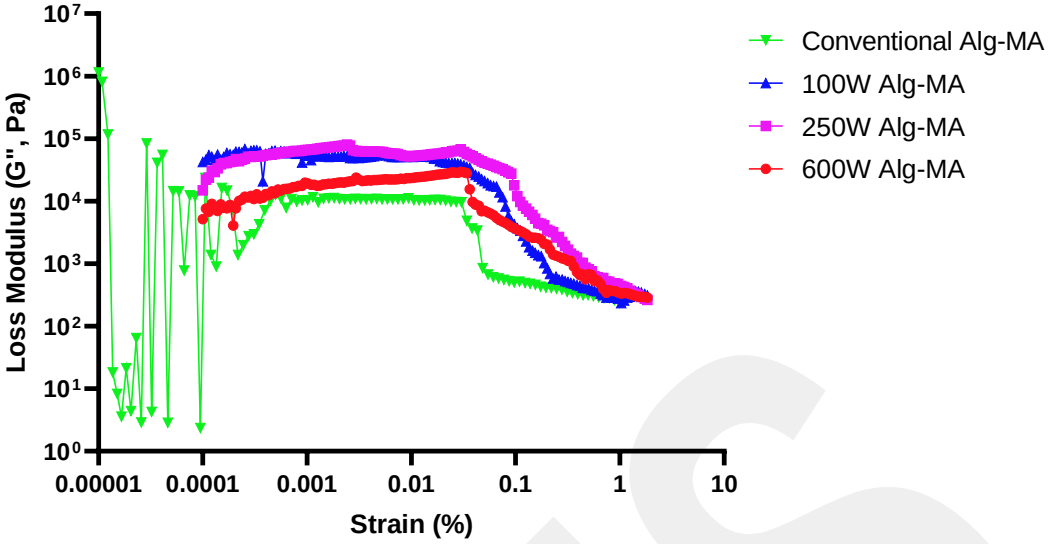

Figure 3.15 Strain-dependent loss modulus of Alg-MA hydrogels after crosslinking.

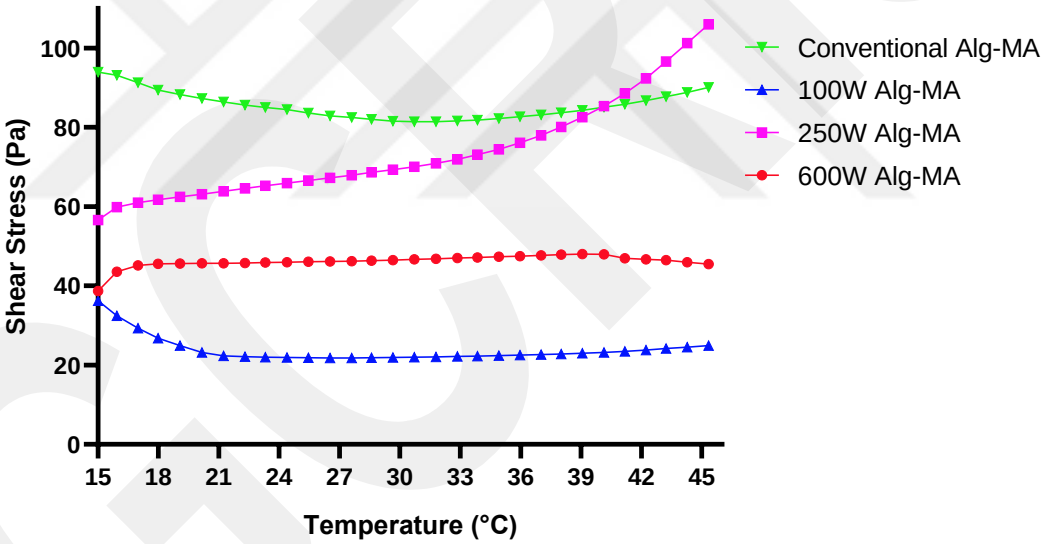

Figure 3.16 Temperature-dependent shear stress of Alg-MA hydrogels after crosslinking.

3.6. SEM Analysis

The morphological structures of hydrogels produced for use in tissue engineering applications are important for cell studies. Pores and their interconnectivity nature is critical for cell attachment, migration and proliferation. In addition, cells can carry the nutrients and oxygen they need, while cell waste can be

removed from the environment. Hydrogels can provide interconnective porous structure due to their architectural characteristics.

In order to examine the surface morphologies, conventional Alg-MA and 250W Alg-MA hydrogel groups were dried in a lyophilisator and then coated with 10 nm gold. Following this, the samples were examined by SEM.

Figure 3.17 shows SEM images of conventional Alg-MA hydrogel groups. When SEM images were investigated, it was seen that all hydrogel groups had a porous structure. When hydrogels with different concentrations were examined (Figure 3.17b, Figure 3.17c), it was observed that the hydrogel containing 5% tannic acid had a more dense porous structure than the hydrogel containing 0.5% tannic acid.

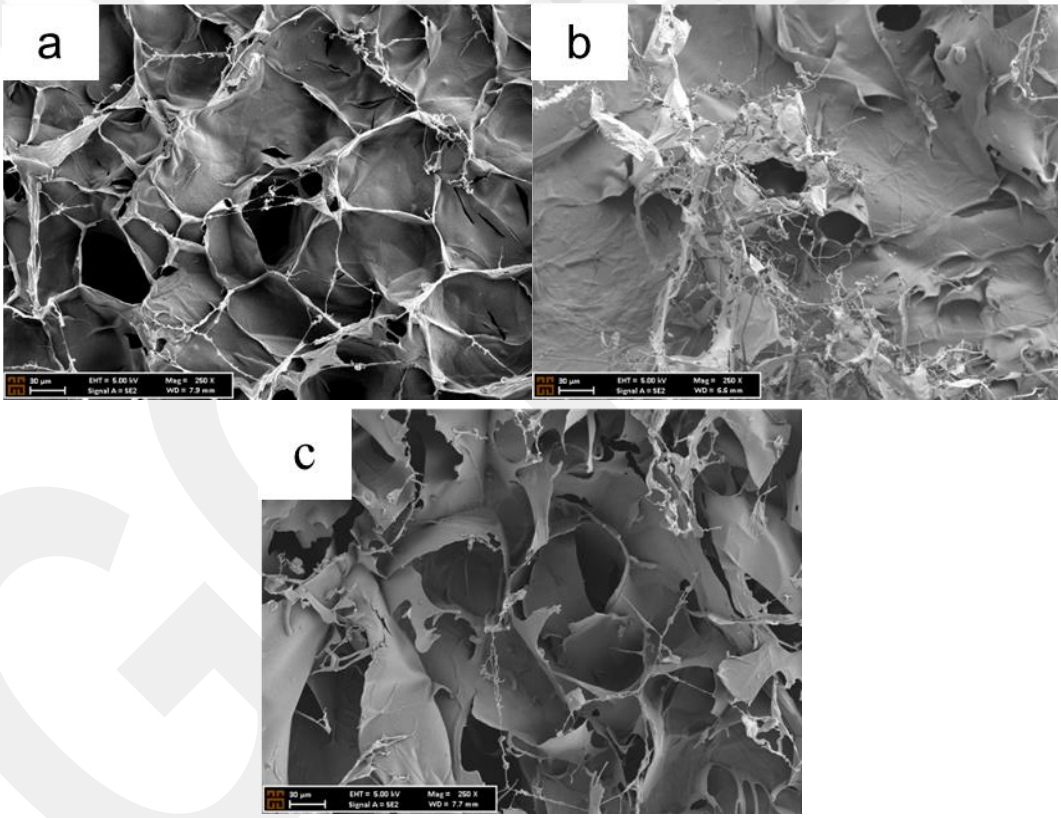

Figure 3.17 SEM images of conventional Alg-MA hydrogels. (a) non-TA, (b) 0.5% TA and (c) 5% TA. All magnification: 250X.

SEM images of 250W Alg-MA hydrogel groups are shown in Figure 3.18. When the figures are examined, it was seen that both the hydrogel without tannic acid (Figure 3.18a) and the hydrogel containing 0.5% tannic acid (Figure 3.18b) had a flat structure. The hydrogel containing 5% tannic acid (Figure 3.18c) was observed to have a porous structure compared to the others.

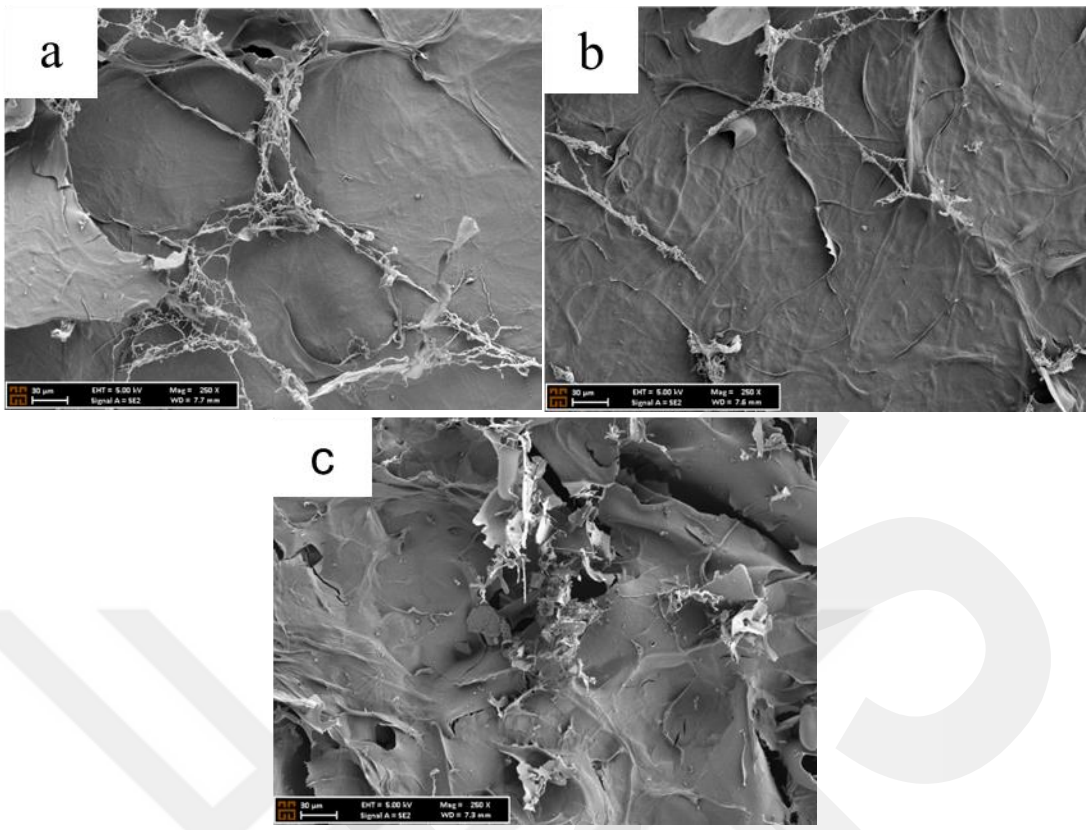

Figure 3.18 SEM images of 250W Alg-MA hydrogels. (a) non-TA, (b) 0.5% TA and (c) 5% TA. All magnification: 250X.

According to these results, the addition of tannic acid contributed positively to the formation of porous structure of hydrogels. In addition, it was observed that the pore formation in the structure of hydrogels increased with the increase of tannic acid concentration, which will provide a supportive feature in the attachment, proliferation and differentiation of cells to hydrogels. In addition, the cells will be involved in the transport of the nutrients and oxygen they need and will help the removal of cell wastes from the environment.

3.7. Swelling and Stability

The change in swelling behaviour represents changes in the physical and chemical structure of the hydrogels [108]. The swelling tests of conventional Alg-MA and 250W Alg-MA hydrogels in PBS for 8 hours are shown in Figure 3.19 and Figure 3.20. In addition, swelling tests were also applied to tannic acid loaded hydrogels (0.5%, 2.5%, 5% TA) in order to examine the effect of tannic acid on the swelling properties of hydrogels. According to the literature, addition of TA is expected to form secondary physical cross-links and give swelling ability to the end product. On

the other hand, a chemically cross-linked hydrogels swelling ability can be restiricted due to these secondary additional cross-links. When Figures 3.19 and 3.20 are examined, it is seen that all samples exhibited very high swelling behaviour within the first 15 minutes and then continued to exhibit swelling behaviour at lower rates for 8 hours. Also, microwave irradiated sample showed a bit more swelling than conventional Alg-MA hydrogel. Also, the non-TA groups showed much more swelling behaviour than the TA groups at different concentrations. Concurrently, as the concentration of tannic acid increased, the swelling behaviour of the hydrogels gradually decreased, which can be attributed to the interaction of the hydrogels with tannic acid promoting the formation of a more stable structure by forming secondary cross-linking [145]. Furthermore, when both figures were examined, it was observed that the TA addition affected the microwave irradiated samples a bit more than the conventional Alg-MA. By microwave irradiation, we obtained better hydrogels as shown by mechanical and rheological analysis , which probably allows more uniform interactions with TA molecules.

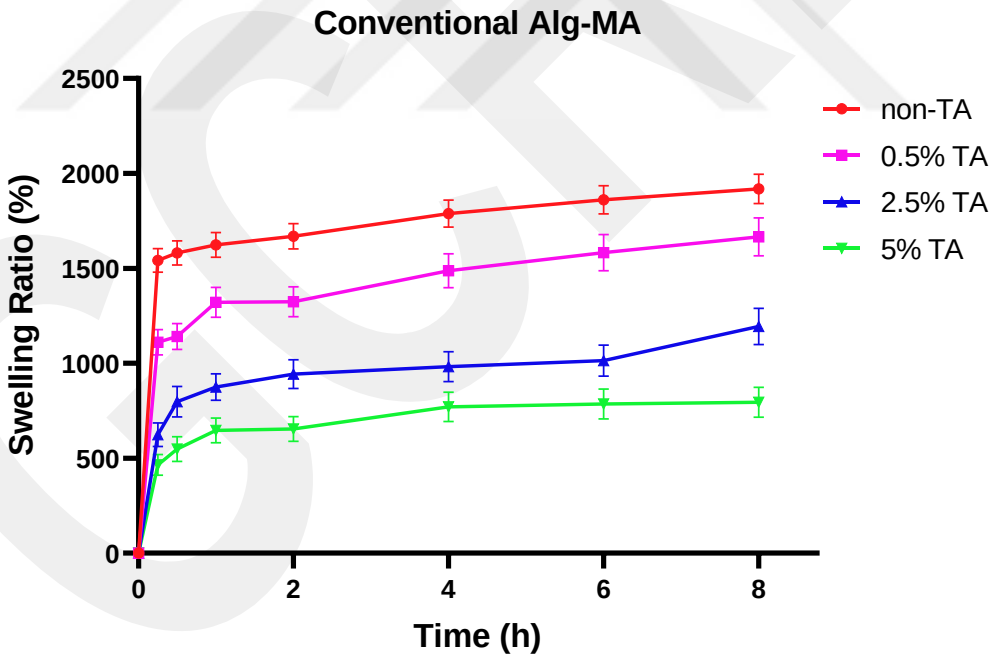

Figure 3.19 Swelling behaviours of conventional Alg-MA hydrogels.

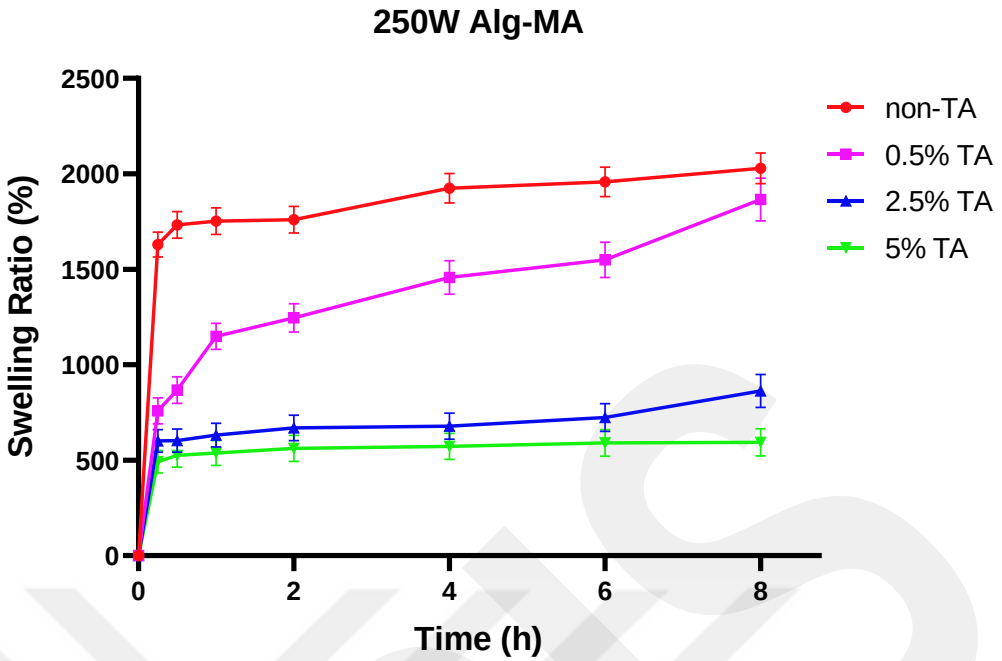

Figure 3.20 Swelling behaviours of 250W Alg-MA hydrogels.

In order to evaluate the stability of hydrogels, TA loaded, conventional Alg-MA and 250W Alg-MA hydrogels were incubated in PBS at 37 ºC for 28 days and samples were taken from media at certain time intervals (3, 7, 14, 21, and 28 days) for weight loss measurement, and results were given in Figure 3.21 and Figure 3.22. First, no wight loss was observed for the hydrogels, which do not contain TA, due to the stability of covalent cross-linking [108]. But, we observed an increasing weight loss in the TA-containing hydrogels, which are proportional to the TA amount in the gels. This was an expected results because physically cross-linked TA molecules had tendency of release from the hydrogels in aqueous medium [151]. Figures 3.21 and 3.22 show that the concentration of tannic acid is directly proportional to the weight loss of the hydrogels because the tannic acid released into the PBS medium depends on the initial concentration of tannic acid in the hydrogels [151]. A burst release of TA was observed in the first 3 days and it was decreased gradually afterwards. Furthermore, no significant difference in weight loss due to tannic acid release was observed between conventional Alg-MA and 250W Alg-MA hydrogels.

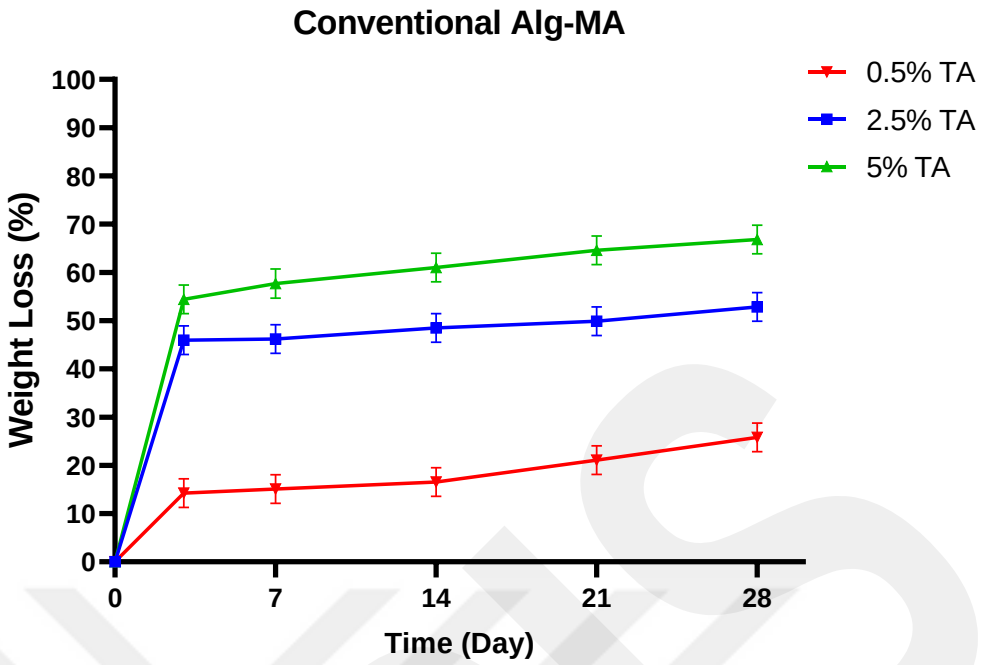

Figure 3.21 Stability properties of conventional Alg-MA hydrogels containing different concentration of TA.

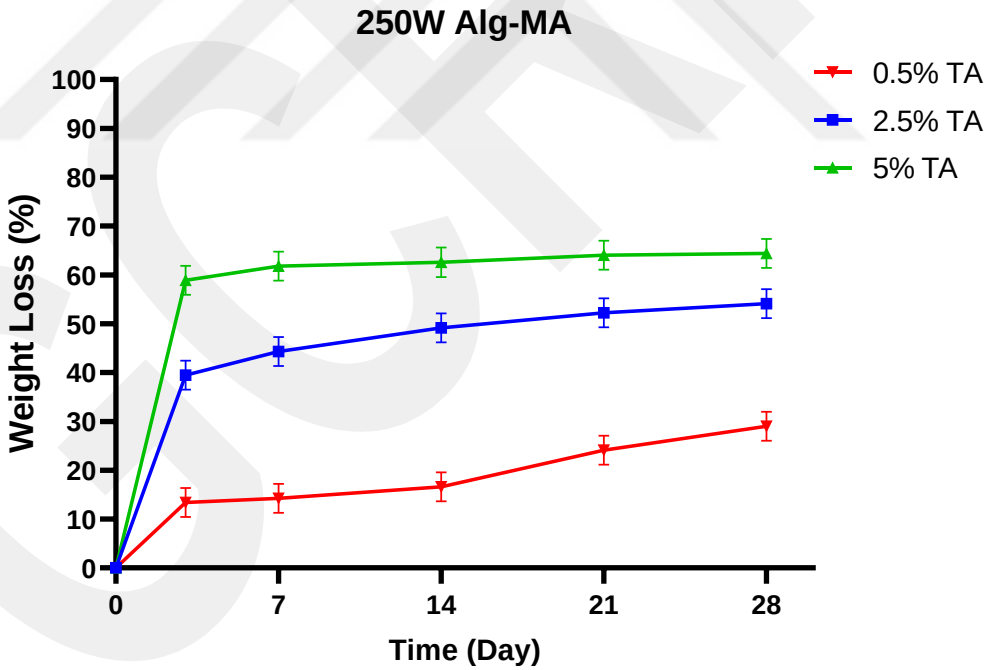

Figure 3.22 Stability properties of 250W Alg-MA hydrogels containing different concentration of TA.

3.8. Antibacterial Activity

Tannic acid (TA) has the ability to trigger cell membrane damage causing cell death and block toxin genes present in bacteria [152]. Therefore, to understand whether TA imparts antibacterial properties to Alg-MA hydrogels, the antibacterial effect of Conventional Alg-MA (C) and 250W Alg-MA (250W) hydrogels containing TA at certain concentrations (0.5%, 2.5%, 5% TA) against Gram-negative (E. coli) and Gram-positive (S. aureus) bacteria was investigated by zone inhibition assay. For each TA concentration, C and 250W hydrogel samples containing antibiotic as positive control, non-TA (blank Alg-MA gel) as negative control and the respective TA concentration were placed on the plates, as shown in Figures 3.23 and 3.24. As expected, the positive control, antibiotics, showed the highest zone diameter, while the negative control, non-TA hydrogels, did not exhibit any antibacterial properties. Moreover, this assay showed that as the TA concentration was increased from 0.5% to 5%, the zone diameters of C and 250W hydrogels increased from 9.4 mm to 16.9 mm and from 9.8 mm to 18.2 mm for E.coli, respectively. Likewise, for S.aureus, it increased from 12.0 mm to 16.9 mm and from 10.1 mm to 16.9 mm, respectively, as shown in Figure 3.25 and 3.26. Furthermore, no significant increase was observed in the zone diameters of Alg-MA hydrogels containing 2.5 and 5% TA, nor between C and 250W hydrogels containing the same concentration of TA. It was realised that the hydrogels containing TA exhibited greater zone diameters against S.aureus than against E.coli. This is because S.aureus is more susceptible to TA due to the ability of TA components to bind directly to the peptidoglycan layer [153]. In conclusion, TA-containing Alg-MA hydrogels showed antibacterial properties against both bacterial species.

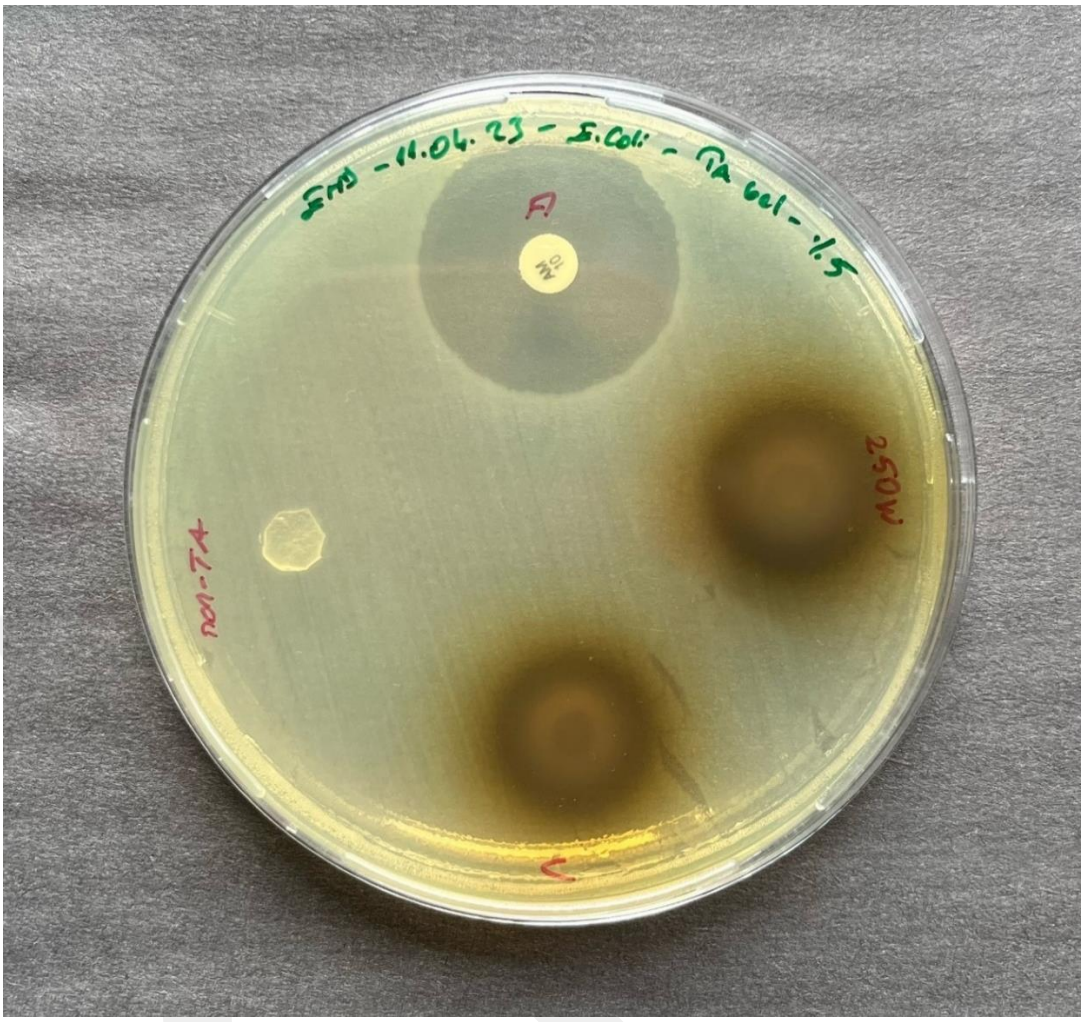

Figure 3.23 Digital image of Alg-MA hydrogels containing 5% TA concentration against E.coli.

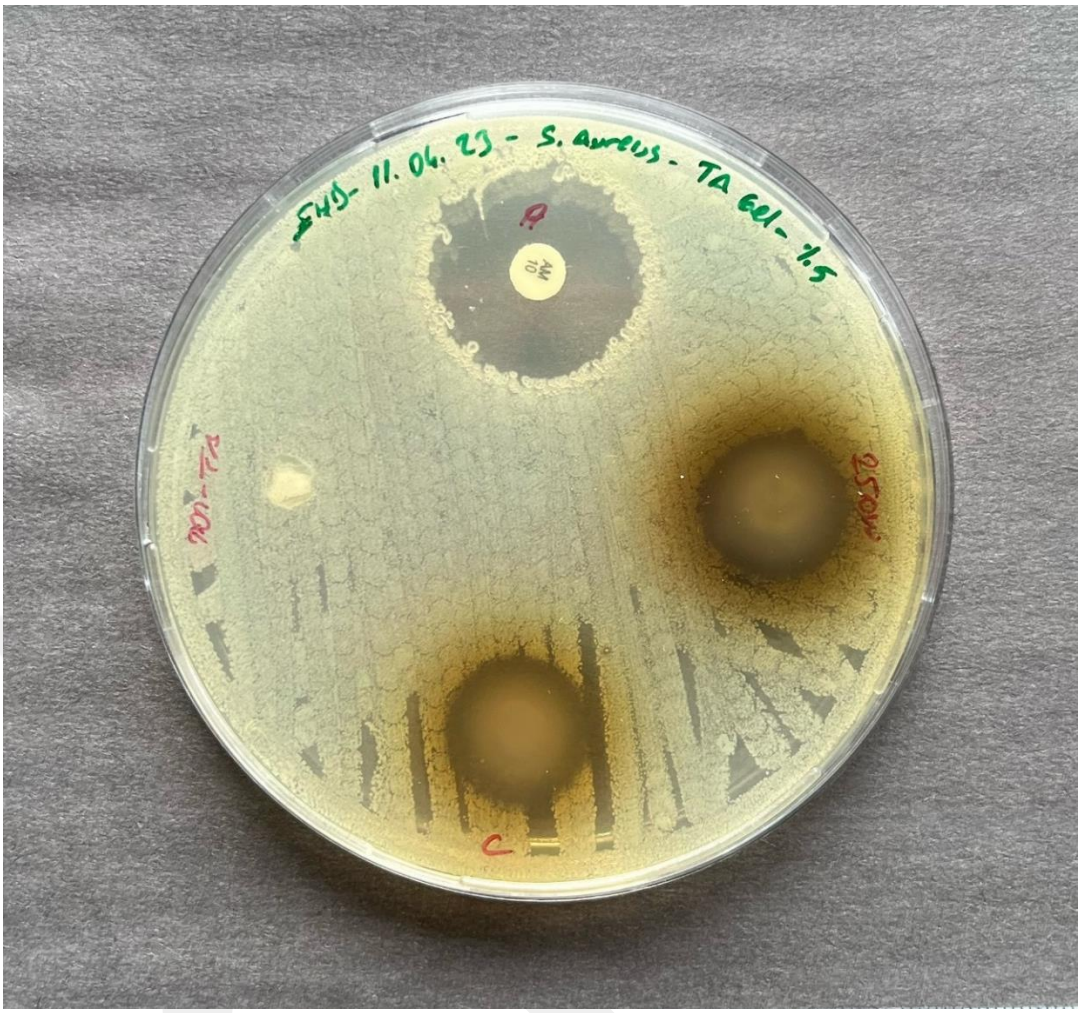

Figure 3.24 Digital image of Alg-MA hydrogels containing 5% TA concentration against S.aureus.

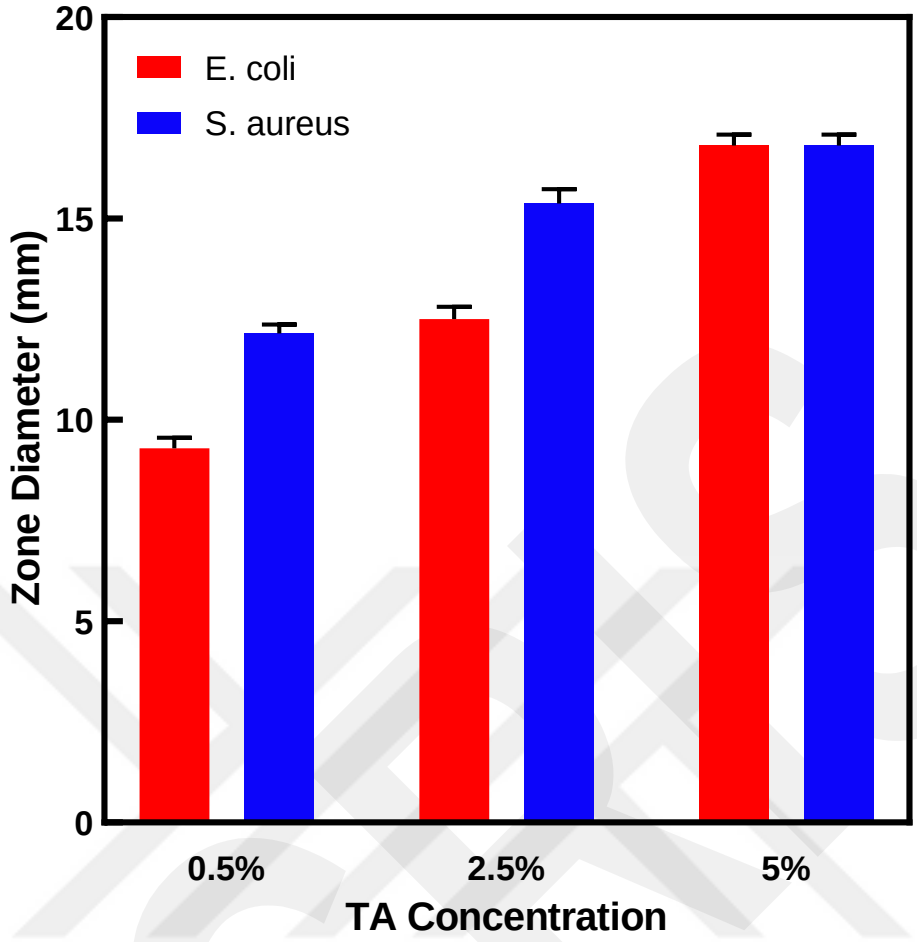

Figure 3.25 Zone diameters (mm) of C hydrogels against E.coli and S.aureus.

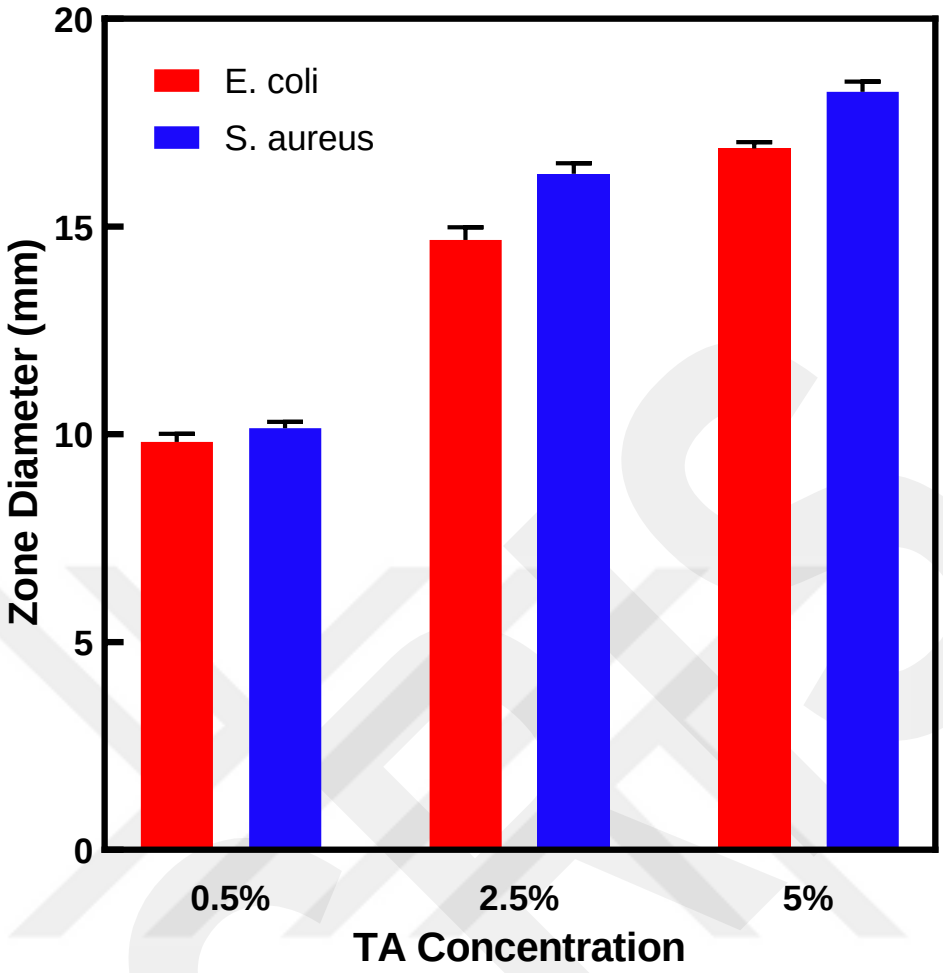

Figure 3.26 Zone diameters (mm) of 250W hydrogels against E.coli and S.aureus.

Chapter 4

4.Conclusions and Future Prospects

4.1. Conclusions

The primary objective of this thesis is to develop Alg-MA with better mechanical characteristics for a potential use as bioinks [154]. In this direction, methacrylated alginates were obtained by reacting alginate (Alg) with 2-aminoethyl methacrylate hydrochloride (AEMA) carbodiimide coupling. We aimed to compare the efficiencies of conventional method and microwave-assisted reaction in terms of degree of methacrylation and reaction time. Our ^{1}H-NMR results showed that higher methacrylation degree was achieved by microwave energy with shorter reaction time. Then, we optimized the printing conditions of Alg-MA hydrogels and found that 5 mm/s printing speed for 4 psi pressure and 10 mm/s printing speed for 6 psi pressure allowed appropriate fibers. In addition, Alg-MA hydrogels were found to have suitable viscosities for bioprinting, according to the rheological analysis. Mechanical test analyses showed that 250W-irradiated Alg-MA hydrogels with the highest methacrylation degree revealed higher deformation resistance with 8.3 kPa compared to the other samples, indicating that more robust hydrogels can be obtained by microwave method than conventional method. Moreover, TA provided hydrogels extra mechanical strength by secondary cross-links. TA addition was also confirmed by FTIR. According to the frequency dependent rheological analysis, the storage modulus of conventional Alg-MA, 100W Alg-MA, 250W Alg-MA, and 600W Alg-MA hydrogel groups at 100rad/s were found to be 39.7 kPa, 50.6 kPa, 45.5 kPa, and 39.9 kPa, respectively. Also, the loss modulus of these hydrogels was found as 0.9 kPa, 2.0 kPa, 1.5 kPa, and 0.7 kPa, respectively. In the literature, the storage modulus (at 100 rad/s) of microwave-assisted GelMA hydrogels (600W/8% MA, 1000W/8% MA, 600W/4% MA, 1000W/4% MA) were obtained as 9 kPa, 39.1 kPa, 27.5 kPa and

41.1 kPa, respectively [155]. The loss modulus of all hydrogels was reported as 0.1 kPa. Based on these findings, Alg-MA hydrogels obtained in our study exhibited higher viscoelastic properties compared to GelMA hydrogels frequently used in the literature. Also, these hydrogels showed a significant swelling behaviour in PBS at 37 oC as expected. Addition of TA limited and decreased the swelling ability of the hydrogels as reported in the literature. The stability of these hydrogels were proved by stability experiment in physiological conditions. We expect antibacterial activity due to TA, therefore we applied antimicrobial test and obtained that TA immersed Alg-MA hydrogels gained antimicrobial characteristics against both Gram-positive and Gram-negative bacteria. As a conclusion, for the first time in the literature, Alg-MAs with higher DM were obtained by microwave irradiated methacrylation synthesis with AEMA. Thanks to the methacrylation process and TA addition, the mechanical properties of alginate were improved. These Alg-MAs containing TA have great potential for use in bioprinting applications as bioinks.

4.2. Societal Impact and Contribution to Global Sustainability

Tissue engineering and regenerative medicine is a field where very important developments in human health are experienced today. According to the data in the USA, although the expenditures on organ transplantation have exceeded millions of dollars, hundreds of thousands of patients are still waiting for a suitable organ to sustain their lives. Due to the current inadequacies in this field, investments and research have accelerated in the production of tissues or organs needed by patients in the laboratory environment and implanting them to the patient. Since the 1990s, many simple tissues and organs such as cartilage, skin and urethra can be obtained in the laboratory environment with the help of a tissue scaffold without using any printing method. However, studies show that there is a great need for large-scale and mass production in this field. Based on this, a urinary bladder was first made with 3D bioprinting in the early 2000s and implanted into the patient. With this important development, the 3D bioprinting technique has enabled the printing of simple organs such as skin as the first category, hollow tubular structures such as vessels as the second category, and hollow but not tubular organs (such as the urinary bladder) as

the third category. Since organs such as the heart, kidney and liver are the most complex, studies on these organs are still ongoing. Currently, under the leadership of Prof. Atala, 3D printing studies are being carried out for 40 different body parts at the Wake Forest Institute for Regenerative Medicine (WFIRM). The fact that the tissue substitutes or organs needed by patients are made using their own cells in the laboratory environment both reduces the dependence on organ transplantation and minimizes the possibility of tissue rejection. It is stated in many studies and articles that this technology is of great importance in terms of personalized medicine. In the light of all this information, within the scope of Turkey's 11th Development Plan, more studies should be carried out using 3D bioprinting technology, which continues to increase rapidly in the field of tissue engineering in recent years in order to move our country to higher levels in international competition. For this purpose, this thesis study on the production and characterisation of alginate-based 3D tissue scaffolds in the field of tissue engineering and regenerative medicine will contribute to the society in terms of improving human health by enabling the formation of a new generation tissue scaffold with increased biocompatibility and and better mechanical properties.

4.3. Future Prospects

The human body consists of many complex systems. These systems contain different tissue and organ structures within themselves. These structures have the ability to regenerate and repair themselves at a certain level. However, due to internal or external factors such as aging or accidental damage, this regeneration/repair ability may be completely lost or a sufficient point may not be reached to perform this process. At this point, scaffold-based approaches in tissue engineering come to the fore in order to replace or regenerate damaged tissues or organs. In addition, three-dimensional bioprinting, which has emerged as a new technology in this field, has made significant progress in recent years and has become an interesting tissue scaffold production method. Based on this, the prepared Alg-MA hydrogels have great potential to be used in bioprinting applications. For the future studies, 3D printing will be applied in the presence of the alive cells and the ECM capabilities of these gels will be investigated by in vitro cell cultures within the scope of high quality and funded research projects. These studies will be followed by animal experiments with specific disease and appripriate scaffold models.

BIBLIOGRAPHY

[1] M. N. Helder, M. Knippenberg, J. Klein-Nulend, and P. I. J. M. Wuisman, 'Stem Cells from Adipose Tissue Allow Challenging New Concepts for Regenerative Medicine', *Tissue Eng*, vol. 13, no. 8, pp. 1799–1808, Aug. 2007, doi: 10.1089/ten.2006.0165.

[2] R. Dai, Z. Wang, R. Samanipour, K. Koo, and K. Kim, 'Adipose-Derived Stem Cells for Tissue Engineering and Regenerative Medicine Applications', *Stem Cells Int*, vol. 2016, pp. 1–19, 2016, doi: 10.1155/2016/6737345.

[3] E. Sheehy *et al.*, 'to Ms. Sheehy at the Association of Organ Procurement Organizations, 1364 Beverly Rd., Suite 100, McLean, VA 22101, or at organdonation@aopo.org', 2003. [Online]. Available: www.nejm.org

[4] R. Langer and J. P. Vacanti, 'Tissue Engineering'. [Online]. Available: www.sciencemag.org

[5] D. Howard, L. D. Buttery, K. M. Shakesheff, and S. J. Roberts, 'Tissue engineering: Strategies, stem cells and scaffolds', *Journal of Anatomy*, vol. 213, no. 1. pp. 66–72, Jul. 2008. doi: 10.1111/j.1469-7580.2008.00878.x.

[6] F. E. Freeman and D. J. Kelly, 'Tuning alginate bioink stiffness and composition for controlled growth factor delivery and to spatially direct MSC Fate within bioprinted tissues', *Sci Rep*, vol. 7, no. 1, Dec. 2017, doi: 10.1038/s41598-017-17286-1.

[7] J. Malda *et al.*, '25th anniversary article: Engineering hydrogels for biofabrication', *Advanced Materials*, vol. 25, no. 36. pp. 5011–5028, Sep. 2013. doi: 10.1002/adma.201302042.

[8] F. P. W. Melchels, M. A. N. Domingos, T. J. Klein, J. Malda, P. J. Bartolo, and D. W. Hutmacher, 'Additive manufacturing of tissues and organs', *Progress in Polymer Science*, vol. 37, no. 8. Elsevier Ltd, pp. 1079–1104, 2012. doi: 10.1016/j.progpolymsci.2011.11.007.

[9] F. Pahlevanzadeh *et al.*, 'Recent trends in three-dimensional bioinks based on alginate for biomedical applications', *Materials*, vol. 13, no. 18, Sep. 2020, doi: 10.3390/ma13183980.

[10] R. 'Ellam, 'Editor's pick: 3D printing: you read it here first', *New Scientist*, Nov. 12, 2016. Accessed: Mar. 01, 2023. [Online]. Available: https://www.newscientist.com/letter/mg23230991-100-1-editors-pick-3d-printing-you-read-it-here-first/

[11] H. Kodama, 'Automatic method for fabricating a three-dimensional plastic model with photo-hardening polymer', *Review of Scientific Instruments*, vol. 52, no. 11, pp. 1770–1773, 1981, doi: 10.1063/1.1136492.

[12] T. de P. L. Lima, C. A. d. A. Canelas, V. O. C. Concha, F. A. M. da Costa, and M. F. Passos, '3D Bioprinting Technology and Hydrogels Used in the Process', *Journal of Functional Biomaterials*, vol. 13, no. 4. MDPI, Dec. 01, 2022. doi: 10.3390/jfb13040214.

[13] Z. Xie, M. Gao, A. O. Lobo, and T. J. Webster, '3D bioprinting in tissue engineering for medical applications: The classic and the hybrid', *Polymers*, vol. 12, no. 8. MDPI AG, Aug. 01, 2020. doi: 10.3390/POLYM12081717.

[14] C. Norotte, F. S. Marga, L. E. Niklason, and G. Forgacs, 'Scaffold-free vascular tissue engineering using bioprinting', *Biomaterials*, vol. 30, no. 30, pp. 5910–5917, Oct. 2009, doi: 10.1016/j.biomaterials.2009.06.034.

[15] S. Ramasamy *et al.*, 'Optimized construction of a full thickness human skin equivalent using 3D bioprinting and a PCL/collagen dermal scaffold', *Bioprinting*, vol. 21, Mar. 2021, doi: 10.1016/j.bprint.2020.e00123.

[16] X. Ma *et al.*, '3D bioprinting of functional tissue models for personalized drug screening and in vitro disease modeling', *Adv Drug Deliv Rev*, vol. 132, pp. 235–251, Jul. 2018, doi: 10.1016/j.addr.2018.06.011.

[17] C. Mandrycky, Z. Wang, K. Kim, and D. H. Kim, '3D bioprinting for engineering complex tissues', *Biotechnology Advances*, vol. 34, no. 4. Elsevier Inc., pp. 422–434, Jul. 01, 2016. doi: 10.1016/j.biotechadv.2015.12.011.

[18] Y. S. Zhang, R. Oklu, M. R. Dokmeci, and A. Khademhosseini, 'Three-dimensional bioprinting strategies for tissue engineering', *Cold Spring Harb Perspect Med*, vol. 8, no. 2, Feb. 2018, doi: 10.1101/cshperspect.a025718.

[19] Y. S. Zhang, M. Duchamp, R. Oklu, L. W. Ellisen, R. Langer, and A. Khademhosseini, 'Bioprinting the Cancer Microenvironment', *ACS Biomaterials Science and Engineering*, vol. 2, no. 10. American Chemical Society, pp. 1710–1721, Oct. 10, 2016. doi: 10.1021/acsbiomaterials.6b00246.

[20] M. Chieruzzi *et al.*, 'Nanomaterials for tissue engineering in dentistry', *Nanomaterials*, vol. 6, no. 7. MDPI AG, Jul. 21, 2016. doi: 10.3390/nano6070134.

[21] Y. Li and C. Liu, 'Nanomaterial-based bone regeneration', *Nanoscale*, vol. 9, no. 15. Royal Society of Chemistry, pp. 4862–4874, Apr. 21, 2017. doi: 10.1039/c7nr00835j.

[22] S. Vijayavenkataraman, W. C. Yan, W. F. Lu, C. H. Wang, and J. Y. H. Fuh, '3D bioprinting of tissues and organs for regenerative medicine', *Advanced Drug Delivery Reviews*, vol. 132. Elsevier B.V., pp. 296–332, Jul. 01, 2018. doi: 10.1016/j.addr.2018.07.004.

[23] 'Review Bioprinting A Beginning'.

[24] V. Mironov, V. Kasyanov, and R. R. Markwald, 'Organ printing: From bioprinter to organ biofabrication line', *Current Opinion in Biotechnology*, vol. 22, no. 5. pp. 667–673, Oct. 2011. doi: 10.1016/j.copbio.2011.02.006.

[25] J. Jia *et al.*, 'Engineering alginate as bioink for bioprinting', *Acta Biomater*, vol. 10, no. 10, pp. 4323–4331, Oct. 2014, doi: 10.1016/j.actbio.2014.06.034.

[26] F. Xing, Z. Xiang, P. M. Rommens, and U. Ritz, '3D bioprinting for vascularized tissue-engineered bone fabrication', *Materials*, vol. 13, no. 10. MDPI AG, May 01, 2020. doi: 10.3390/ma13102278.

[27] S. Agarwal, S. Saha, V. K. Balla, A. Pal, A. Barui, and S. Bodhak, 'Current Developments in 3D Bioprinting for Tissue and Organ Regeneration–A Review', *Front Mech Eng*, vol. 6, p. 90, Oct. 2020, doi: 10.3389/FMECH.2020.589171.

[28] T. J. Horn and O. L. A. Harrysson, 'Overview of current additive manufacturing technologies and selected applications', *Sci Prog*, vol. 95, no. 3, pp. 255–282, 2012, doi: 10.3184/003685012X13420984463047.

[29] H. N. Chia and B. M. Wu, 'Recent advances in 3D printing of biomaterials', *J Biol Eng*, vol. 9, no. 1, Mar. 2015, doi: 10.1186/s13036-015-0001-4.

[30] N. Sigaux, L. Pourchet, P. Breton, S. Brosset, A. Louvrier, and C. A. Marquette, '3D Bioprinting:principles, fantasies and prospects', *Journal of Stomatology, Oral and Maxillofacial Surgery*, vol. 120, no. 2. Elsevier Masson SAS, pp. 128–132, Apr. 01, 2019. doi: 10.1016/j.jormas.2018.12.014.

[31] Ž. P. Kačarević *et al.*, 'An introduction to 3D bioprinting: Possibilities, challenges and future aspects', *Materials*, vol. 11, no. 11. MDPI AG, Nov. 06, 2018. doi: 10.3390/ma11112199.

[32] 'Biocompatible Inkjet Printing Technique for Designed Seeding of Individual Living Cells'.

[33] A. B. Dababneh and I. T. Ozbolat, 'Bioprinting Technology: A Current State-of-the-Art Review', *Journal of Manufacturing Science and Engineering, Transactions of the ASME*, vol. 136, no. 6, Dec. 2014, doi: 10.1115/1.4028512.

[34] S. V. Murphy and A. Atala, '3D bioprinting of tissues and organs', *Nature Biotechnology*, vol. 32, no. 8. Nature Publishing Group, pp. 773–785, 2014. doi: 10.1038/nbt.2958.

[35] Z. Xia, S. Jin, and K. Ye, 'Tissue and Organ 3D Bioprinting', *SLAS Technology*, vol. 23, no. 4. SAGE Publications Inc., pp. 301–314, Aug. 01, 2018. doi: 10.1177/2472630318760515.

[36] U. Jammalamadaka and K. Tappa, 'Recent advances in biomaterials for 3D printing and tissue engineering', *Journal of Functional Biomaterials*, vol. 9, no. 1. MDPI AG, Mar. 01, 2018. doi: 10.3390/jfb9010022.

[37] E. Tekin, P. J. Smith, and U. S. Schubert, 'Inkjet printing as a deposition and patterning tool for polymers and inorganic particles', *Soft Matter*, vol. 4, no. 4, pp. 703–713, 2008, doi: 10.1039/b711984d.

[38] C. Tse *et al.*, 'Inkjet printing Schwann cells and neuronal analogue NG108-15 cells', *Biofabrication*, vol. 8, no. 1, 2016, doi: 10.1088/1758-5090/8/1/015017.

[39] S. Agarwal, S. Saha, V. K. Balla, A. Pal, A. Barui, and S. Bodhak, ‘Current Developments in 3D Bioprinting for Tissue and Organ Regeneration–A Review’, *Front Mech Eng*, vol. 6, Oct. 2020, doi: 10.3389/fmech.2020.589171.

[40] S. Jana and A. Lerman, ‘Bioprinting a cardiac valve’, *Biotechnology Advances*, vol. 33, no. 8. Elsevier Inc., pp. 1503–1521, 2015. doi: 10.1016/j.biotechadv.2015.07.006.

[41] J. A. Barron, D. B. Krizman, and B. R. Ringeisen, ‘Laser printing of single cells: Statistical analysis, cell viability, and stress’, *Ann Biomed Eng*, vol. 33, no. 2, pp. 121–130, Feb. 2005, doi: 10.1007/s10439-005-8971-x.

[42] V. Keriquel *et al.*, ‘In situ printing of mesenchymal stromal cells, by laser-assisted bioprinting, for in vivo bone regeneration applications’, *Sci Rep*, vol. 7, no. 1, Dec. 2017, doi: 10.1038/s41598-017-01914-x.

[43] M. Gruene *et al.*, ‘Laser printing of stem cells for biofabrication of scaffold-free autologous grafts’, *Tissue Eng Part C Methods*, vol. 17, no. 1, pp. 79–87, Aug. 2010, doi: 10.1089/ten.tec.2010.0359.

[44] I. T. Ozbolat and Y. Yu, ‘Bioprinting toward organ fabrication: Challenges and future trends’, *IEEE Trans Biomed Eng*, vol. 60, no. 3, pp. 691–699, 2013, doi: 10.1109/TBME.2013.2243912.

[45] ‘Progress in Additive Manufacturing and Rapid Prototyping’.

[46] I. Gibson, D. Rosen, and B. Stucker, *Additive manufacturing technologies: 3D printing, rapid prototyping, and direct digital manufacturing, second edition*. Springer New York, 2015. doi: 10.1007/978-1-4939-2113-3.

[47] P. Mohan Pandey, N. Venkata Reddy, and S. G. Dhande, ‘Slicing procedures in layered manufacturing: A review’, *Rapid Prototyp J*, vol. 9, no. 5, pp. 274–288, Dec. 2003, doi: 10.1108/13552540310502185.

[48] S. M. Peltola, F. P. W. Melchels, D. W. Grijpma, and M. Kellomäki, ‘A review of rapid prototyping techniques for tissue engineering purposes’, *Annals of Medicine*, vol. 40, no. 4. pp. 268–280, 2008. doi: 10.1080/07853890701881788.

[49] F. You, B. F. Eames, and X. Chen, ‘Application of extrusion-based hydrogel bioprinting for cartilage tissue engineering’, *International Journal of Molecular Sciences*, vol. 18, no. 7. MDPI AG, Jul. 23, 2017. doi: 10.3390/ijms18071597.

[50] V. Mironov, T. Trusk, V. Kasyanov, S. Little, R. Swaja, and R. Markwald, ‘Biofabrication: A 21st century manufacturing paradigm’, *Biofabrication*, vol. 1, no. 2. 2009. doi: 10.1088/1758-5082/1/2/022001.

[51] I. T. Ozbolat, ‘Scaffold-Based or Scaffold-Free Bioprinting: Competing or Complementing Approaches?’, *J Nanotechnol Eng Med*, vol. 6, no. 2, May 2015, doi: 10.1115/1.4030414.

[52] I. T. Ozbolat and M. Hospodiuk, ‘Current advances and future perspectives in extrusion-based bioprinting’, *Biomaterials*, vol. 76. Elsevier Ltd, pp. 321–343, 2016. doi: 10.1016/j.biomaterials.2015.10.076.

[53] E. Y. S. Tan and W. Y. Yeong, ‘Concentric bioprinting of alginate-based tubular constructs using multi-nozzle extrusion-based technique’, *Int J Bioprint*, vol. 1, no. 1, pp. 49–56, 2015, doi: 10.18063/IJB.2015.01.003.

[54] F. Dolati, Y. Yu, Y. Zhang, A. M. D. Jesus, E. A. Sander, and I. T. Ozbolat, ‘In vitro evaluation of carbon-nanotube-reinforced bioprintable vascular conduits’, *Nanotechnology*, vol. 25, no. 14, Apr. 2014, doi: 10.1088/0957-4484/25/14/145101.

[55] P. S. Gungor-Ozkerim, I. Inci, Y. S. Zhang, A. Khademhosseini, and M. R. Dokmeci, ‘Bioinks for 3D bioprinting: An overview’, *Biomaterials Science*, vol. 6, no. 5. Royal Society of Chemistry, pp. 915–946, May 01, 2018. doi: 10.1039/c7bm00765e.

[56] K. Hölzl, S. Lin, L. Tytgat, S. Van Vlierberghe, L. Gu, and A. Ovsianikov, ‘Bioink properties before, during and after 3D bioprinting’, *Biofabrication*, vol. 8, no. 3. Institute of Physics Publishing, Sep. 23, 2016. doi: 10.1088/1758-5090/8/3/032002.

[57] J. Groll *et al.*, ‘Biofabrication: Reappraising the definition of an evolving field’, *Biofabrication*, vol. 8, no. 1. Institute of Physics Publishing, Jan. 08, 2016. doi: 10.1088/1758-5090/8/1/013001.

[58] R. Langer and J. P. Vacanti, ‘Tissue Engineering’. [Online]. Available: www.sciencemag.org

[59] K. Y. Lee and D. J. Mooney, ‘Hydrogels for tissue engineering’, *Chemical Reviews*, vol. 101, no. 7. pp. 1869–1879, Jul. 2001. doi: 10.1021/cr000108x.

[60] V. Mironov, R. P. Visconti, V. Kasyanov, G. Forgacs, C. J. Drake, and R. R. Markwald, ‘Organ printing: Tissue spheroids as building blocks’, *Biomaterials*, vol. 30, no. 12, pp. 2164–2174, Apr. 2009, doi: 10.1016/j.biomaterials.2008.12.084.

[61] L. Moroni *et al.*, ‘Biofabrication: A Guide to Technology and Terminology’, *Trends in Biotechnology*, vol. 36, no. 4. Elsevier Ltd, pp. 384–402, Apr. 01, 2018. doi: 10.1016/j.tibtech.2017.10.015.

[62] J. Groll *et al.*, ‘A definition of bioinks and their distinction from biomaterial inks’, *Biofabrication*, vol. 11, no. 1. Institute of Physics Publishing, Jan. 01, 2019. doi: 10.1088/1758-5090/aaec52.

[63] D. G. Tamay and N. Hasirci, ‘Bioinks—materials used in printing cells in designed 3D forms’, *Journal of Biomaterials Science, Polymer Edition*, vol. 32, no. 8. Bellwether Publishing, Ltd., pp. 1072–1106, 2021. doi: 10.1080/09205063.2021.1892470.

[64] S. Ji and M. Guvendiren, ‘Recent Advances in Bioink Design for 3D Bioprinting of Tissues and Organs’, *Frontiers in Bioengineering and Biotechnology*, vol. 5, no. APR. Frontiers Media S.A., Apr. 05, 2017. doi: 10.3389/fbioe.2017.00023.

[65] J. Gopinathan and I. Noh, ‘Recent trends in bioinks for 3D printing’, *Biomaterials Research*, vol. 22, no. 1. BioMed Central Ltd., Apr. 06, 2018. doi: 10.1186/s40824-018-0122-1.

[66] Y. Li and E. Kumacheva, ‘A P P L I E D S C I E N C E S A N D E N G I N E E R I N G Hydrogel microenvironments for cancer spheroid growth and drug screening’, 2018.

[67] A. S. Hoffman, ‘Hydrogels for biomedical applications’, *Advanced Drug Delivery Reviews*, vol. 64, no. SUPPL. pp. 18–23, Dec. 2012. doi: 10.1016/j.addr.2012.09.010.

[68] D. Seliktar, ‘Designing cell-compatible hydrogels for biomedical applications’, *Science*, vol. 336, no. 6085. American Association for the Advancement of Science, pp. 1124–1128, Jun. 01, 2012. doi: 10.1126/science.1214804.

[69] N. A. Peppas and E. W. Merrill, ‘Crosslinked Poly(vinyl Alcohol) Hydrogels as Swollen Elastic Networks’, 1977.

[70] J. Kopeĉek, ‘Hydrogels: From soft contact lenses and implants to self-assembled nanomaterials’, *J Polym Sci A Polym Chem*, vol. 47, no. 22, pp. 5929–5946, Nov. 2009, doi: 10.1002/pola.23607.

[71] A. Sannino, C. Demitri, and M. Madaghiele, ‘Biodegradable cellulose-based hydrogels: Design and applications’, *Materials*, vol. 2, no. 2. pp. 353–373, 2009. doi: 10.3390/ma2020353.

[72] F. Marga *et al.*, ‘Toward engineering functional organ modules by additive manufacturing’, *Biofabrication*, vol. 4, no. 2. Jun. 2012. doi: 10.1088/1758-5082/4/2/022001.

[73] J. Yu *et al.*, ‘Current advances in 3D bioprinting technology and its applications for tissue engineering’, *Polymers*, vol. 12, no. 12. MDPI AG, pp. 1–30, Dec. 01, 2020. doi: 10.3390/polym12122958.

[74] Z. Li and M. Kawashita, ‘Current progress in inorganic artificial biomaterials’, *Journal of Artificial Organs*, vol. 14, no. 3. pp. 163–170, Sep. 2011. doi: 10.1007/s10047-011-0585-5.

[75] K. L. Spiller, S. A. Maher, and A. M. Lowman, ‘Hydrogels for the repair of articular cartilage defects’, *Tissue Eng Part B Rev*, vol. 17, no. 4, pp. 281–299, Aug. 2011, doi: 10.1089/ten.teb.2011.0077.

[76] N. C. Hunt and L. M. Grover, ‘Cell encapsulation using biopolymer gels for regenerative medicine’, *Biotechnology Letters*, vol. 32, no. 6. pp. 733–742, 2010. doi: 10.1007/s10529-010-0221-0.

[77] K. Y. Lee and D. J. Mooney, ‘Alginate: Properties and biomedical applications’, *Progress in Polymer Science (Oxford)*, vol. 37, no. 1. Elsevier Ltd, pp. 106–126, 2012. doi: 10.1016/j.progpolymsci.2011.06.003.

[78] E. M. Ahmed, ‘Hydrogel: Preparation, characterization, and applications: A review’, *Journal of Advanced Research*, vol. 6, no. 2. Elsevier B.V., pp. 105–121, 2015. doi: 10.1016/j.jare.2013.07.006.

[79] D. B. Kolesky, K. A. Homan, M. A. Skylar-Scott, and J. A. Lewis, ‘Three-dimensional bioprinting of thick vascularized tissues’, *Proc Natl Acad Sci U S A*, vol. 113, no. 12, pp. 3179–3184, Mar. 2016, doi: 10.1073/pnas.1521342113.

[80] A. Skardal and A. Atala, ‘Biomaterials for Integration with 3-D Bioprinting’, *Ann Biomed Eng*, vol. 43, no. 3, pp. 730–746, Mar. 2015, doi: 10.1007/s10439-014-1207-1.

[81] S. Duchi *et al.*, ‘Handheld Co-Axial Bioprinting: Application to in situ surgical cartilage repair’, *Sci Rep*, vol. 7, no. 1, Dec. 2017, doi: 10.1038/s41598-017-05699-x.

[82] J. Li, C. Wu, P. K. Chu, and M. Gelinsky, ‘3D printing of hydrogels: Rational design strategies and emerging biomedical applications’, *Materials Science and Engineering R: Reports*, vol. 140. Elsevier Ltd, Apr. 01, 2020. doi: 10.1016/j.mser.2020.100543.

[83] Z. Gu, J. Fu, H. Lin, and Y. He, ‘Development of 3D bioprinting: From printing methods to biomedical applications’, *Asian Journal of Pharmaceutical Sciences*, vol. 15, no. 5. Shenyang Pharmaceutical University, pp. 529–557, Sep. 01, 2020. doi: 10.1016/j.ajps.2019.11.003.

[84] Y. J. Seol, H. W. Kang, S. J. Lee, A. Atala, and J. J. Yoo, ‘Bioprinting technology and its applications’, *European Journal of Cardio-thoracic Surgery*, vol. 46, no. 3. European Association for Cardio-Thoracic Surgery, pp. 342–348, 2014. doi: 10.1093/ejcts/ezu148.

[85] S. Ahn, H. Lee, L. J. Bonassar, and G. Kim, ‘Cells (MC3T3-E1)-laden alginate scaffolds fabricated by a modified solid-freeform fabrication process supplemented with an aerosol spraying’, *Biomacromolecules*, vol. 13, no. 9, pp. 2997–3003, Sep. 2012, doi: 10.1021/bm3011352.

[86] ‘Direct freeform fabrication of seeded hydrogels in arbitrary geometries’.

[87] N. E. Fedorovich *et al.*, ‘Biofabrication of osteochondral tissue equivalents by printing topologically defined, cell-laden hydrogel scaffolds’, *Tissue Eng Part C Methods*, vol. 18, no. 1, pp. 33–44, Jan. 2012, doi: 10.1089/ten.tec.2011.0060.

[88] D. G. Tamay and N. Hasirci, ‘Bioinks—materials used in printing cells in designed 3D forms’, *Journal of Biomaterials Science, Polymer Edition*, vol. 32, no. 8. Bellwether Publishing, Ltd., pp. 1072–1106, 2021. doi: 10.1080/09205063.2021.1892470.

[89] S. N. Pawar and K. J. Edgar, ‘Alginate derivatization: A review of chemistry, properties and applications’, *Biomaterials*, vol. 33, no. 11. pp. 3279–3305, Apr. 2012. doi: 10.1016/j.biomaterials.2012.01.007.

[90] K. I. Draget, G. Skjåk-Braek, and O. Smidsrød, ‘Alginate based new materials’, 1997.

[91] J. L. Drury and D. J. Mooney, ‘Hydrogels for tissue engineering: Scaffold design variables and applications’, *Biomaterials*, vol. 24, no. 24. Elsevier BV, pp. 4337–4351, 2003. doi: 10.1016/S0142-9612(03)00340-5.

[92] J. Dumbleton *et al.*, ‘The Effect of RGD Peptide on 2D and Miniaturized 3D Culture of HEPM Cells, MSCs, and ADSCs with Alginate Hydrogel’, *Cell Mol Bioeng*, vol. 9, no. 2, pp. 277–288, Jun. 2016, doi: 10.1007/s12195-016-0428-9.

[93] M. Saquib Hasnain *et al.*, ‘Alginates Versatile Polymers in Biomedical Applications and Therapeutics Chemically Modified Alginates for Advanced Biomedical Applications Alginates Versatile Polymers in Biomedical Applications and Therapeutics Chemically Modified Alginates for Advanced Biomedical Applications New Book Announcement’, 2019. [Online]. Available: https://www.researchgate.net/publication/331260652

[94] B. Balakrishnan, N. Joshi, A. Jayakrishnan, and R. Banerjee, ‘Self-crosslinked oxidized alginate/gelatin hydrogel as injectable, adhesive biomimetic scaffolds for cartilage regeneration’, *Acta Biomater*, vol. 10, no. 8, pp. 3650–3663, 2014, doi: 10.1016/j.actbio.2014.04.031.

[95] L. Raddatz *et al.*, ‘Development and application of an additively manufactured calcium chloride nebulizer for alginate 3D-bioprinting purposes’, *J Funct Biomater*, vol. 9, no. 4, Nov. 2018, doi: 10.3390/jfb9040063.

[96] E. Axpe and M. L. Oyen, ‘Applications of alginate-based bioinks in 3D bioprinting’, *International Journal of Molecular Sciences*, vol. 17, no. 12. MDPI AG, Dec. 01, 2016. doi: 10.3390/ijms17121976.

[97] Q. Gao, B. S. Kim, and G. Gao, ‘Advanced Strategies for 3D Bioprinting of Tissue and Organs Analogs Using Alginate Hydrogel Bioinks’, *Marine Drugs*, vol. 19, no. 12. MDPI, Dec. 01, 2021. doi: 10.3390/md19120708.

[98] Y. Zhang, Y. Yu, H. Chen, and I. T. Ozbolat, ‘Characterization of printable cellular micro-fluidic channels for tissue engineering’, *Biofabrication*, vol. 5, no. 2, Jun. 2013, doi: 10.1088/1758-5082/5/2/025004.

[99] Y. Yu, Y. Zhang, J. A. Martin, and I. T. Ozbolat, ‘Evaluation of cell viability and functionality in vessel-like bioprintable cell-laden tubular channels’, *J Biomech Eng*, vol. 135, no. 9, 2013, doi: 10.1115/1.4024575.

[100] Q. Gao, Y. He, J. zhong Fu, A. Liu, and L. Ma, ‘Coaxial nozzle-assisted 3D bioprinting with built-in microchannels for nutrients delivery’, *Biomaterials*, vol. 61, pp. 203–215, Aug. 2015, doi: 10.1016/j.biomaterials.2015.05.031.

[101] W. Jia *et al.*, ‘Direct 3D bioprinting of perfusable vascular constructs using a blend bioink’, *Biomaterials*, vol. 106, pp. 58–68, Nov. 2016, doi: 10.1016/j.biomaterials.2016.07.038.

[102] K. Christensen, C. Xu, W. Chai, Z. Zhang, J. Fu, and Y. Huang, 'Freeform inkjet printing of cellular structures with bifurcations', *Biotechnol Bioeng*, vol. 112, no. 5, pp. 1047–1055, May 2015, doi: 10.1002/bit.25501.

[103] L. Ning, Y. Xu, X. Chen, and D. J. Schreyer, 'Influence of mechanical properties of alginate-based substrates on the performance of Schwann cells in culture', *J Biomater Sci Polym Ed*, vol. 27, no. 9, pp. 898–915, Jun. 2016, doi: 10.1080/09205063.2016.1170415.

[104] A. Faulkner-Jones *et al.*, 'Bioprinting of human pluripotent stem cells and their directed differentiation into hepatocyte-like cells for the generation of mini-livers in 3D', *Biofabrication*, vol. 7, no. 4, Oct. 2015, doi: 10.1088/1758-5090/7/4/044102.

[105] Y. Zhao *et al.*, 'Three-dimensional printing of Hela cells for cervical tumor model in vitro', *Biofabrication*, vol. 6, no. 3, 2014, doi: 10.1088/1758-5082/6/3/035001.

[106] T. Ahlfeld *et al.*, 'Development of a clay based bioink for 3D cell printing for skeletal application', *Biofabrication*, vol. 9, no. 3, Jul. 2017, doi: 10.1088/1758-5090/aa7e96.

[107] A. Kosik-Kozioł *et al.*, 'PLA short sub-micron fiber reinforcement of 3D bioprinted alginate constructs for cartilage regeneration', *Biofabrication*, vol. 9, no. 4, Nov. 2017, doi: 10.1088/1758-5090/aa90d7.

[108] O. Jeon, K. H. Bouhadir, J. M. Mansour, and E. Alsberg, 'Photocrosslinked alginate hydrogels with tunable biodegradation rates and mechanical properties', *Biomaterials*, vol. 30, no. 14, pp. 2724–2734, May 2009, doi: 10.1016/j.biomaterials.2009.01.034.

[109] A. D. Rouillard *et al.*, 'Methods for photocrosslinking alginate hydrogel scaffolds with high cell viability', *Tissue Eng Part C Methods*, vol. 17, no. 2, pp. 173–179, Feb. 2011, doi: 10.1089/ten.tec.2009.0582.

[110] K. A. Smeds and M. W. Grinstaff, 'Photocrosslinkable polysaccharides for in situ hydrogel formation', 2000. [Online]. Available: www.chem.duke.edu/

[111] R. H. Schmedlen, K. S. Masters, and J. L. West, 'Photocrosslinkable polyvinyl alcohol hydrogels that can be modified with cell adhesion peptides for use in tissue engineering', 2002.

[112] J. L. Ifkovits and J. A. Burdick, 'Review: Photopolymerizable and degradable biomaterials for tissue engineering applications', *Tissue Engineering*, vol. 13, no. 10. pp. 2369–2385, Oct. 01, 2007. doi: 10.1089/ten.2007.0093.

[113] K. T. Nguyen and J. L. West, 'Photopolymerizable hydrogels for tissue engineering applications', 2002.

[114] M. A. Daniele, D. A. Boyd, A. A. Adams, and F. S. Ligler, 'Microfluidic strategies for design and assembly of microfibers and nanofibers with tissue engineering and regenerative medicine applications', *Adv Healthc Mater*, vol. 4, no. 1, pp. 11–28, Jan. 2015, doi: 10.1002/adhm.201400144.

[115] D. L. Nettles, T. Parker Vail, M. T. Morgan, M. W. Grinstaff, and L. A. Setton, 'Photocrosslinkable Hyaluronan as a Scaffold for Articular Cartilage Repair', 2004.

[116] O. Jeon, C. Powell, S. M. Ahmed, and E. Alsberg, 'Biodegradable, photocrosslinked alginate hydrogels with independently tailorable physical properties and cell adhesivity', *Tissue Eng Part A*, vol. 16, no. 9, pp. 2915–2925, Sep. 2010, doi: 10.1089/ten.tea.2010.0096.

[117] J. Sun *et al.*, 'The development of cell-initiated degradable hydrogel based on methacrylated alginate applicable to multiple microfabrication technologies', *J Mater Chem B*, vol. 5, no. 40, pp. 8060–8069, 2017, doi: 10.1039/c7tb01458a.

[118] A. Boddupalli and K. M. Bratlie, 'Collagen organization deposited by fibroblasts encapsulated in pH responsive methacrylated alginate hydrogels', *J Biomed Mater Res A*, vol. 106, no. 11, pp. 2934–2943, Nov. 2018, doi: 10.1002/jbm.a.36482.

[119] Z. Özdemir, M. Topuzoğullari, I. A. Işoğlu, and S. Dinçer, 'RAFT-mediated synthesis of poly(N-(2-hydroxypropyl)methacrylamide-b-4- vinylpyridine) by conventional and microwave heating', *Polymer Bulletin*, vol. 70, no. 10, pp. 2857–2872, Oct. 2013, doi: 10.1007/s00289-013-0993-1.

[120] N. Illy, M. Robitzer, R. Auvergne, S. Caillol, G. David, and B. Boutevin, 'Synthesis of water-soluble allyl-functionalized oligochitosan and its modification by thiol-ene addition in water', *J Polym Sci A Polym Chem*, vol. 52, no. 1, pp. 39–48, Jan. 2014, doi: 10.1002/pola.26967.

[121] I. G. Beşkardeş, T. T. Demirtaş, M. D. Durukan, and M. Gümüşderelioğlu, 'Microwave-assisted fabrication of chitosan-hydroxyapatite superporous hydrogel composites as bone scaffolds', *J Tissue Eng Regen Med*, vol. 9, no. 11, pp. 1233–1246, Nov. 2015, doi: 10.1002/term.1677.

[122] J. Jing, S. Liang, Y. Yan, X. Tian, and X. Li, 'Fabrication of Hybrid Hydrogels from Silk Fibroin and Tannic Acid with Enhanced Gelation and Antibacterial Activities', *ACS Biomater Sci Eng*, vol. 5, no. 9, pp. 4601–4611, Sep. 2019, doi: 10.1021/acsbiomaterials.9b00604.

[123] H. Onodera *et al.*, '@ Pergamon Research Section STUDY ON THE CARCINOGENICITY OF TANNIC ACID IN F344 RATS', 1994.

[124] D. P. Makris, G. Boskou, and N. K. Andrikopoulos, 'Polyphenolic content and in vitro antioxidant characteristics of wine industry and other agri-food solid waste extracts', *Journal of Food Composition and Analysis*, vol. 20, no. 2, pp. 125–132, Mar. 2007, doi: 10.1016/j.jfca.2006.04.010.

[125] M. Auriemma, A. Piscitelli, R. Pasquino, P. Cerruti, M. Malinconico, and N. Grizzuti, 'Blending poly(3-hydroxybutyrate) with tannic acid: Influence of a polyphenolic natural additive on the rheological and thermal behavior', *Eur Polym J*, vol. 63, pp. 123–131, 2015, doi: 10.1016/j.eurpolymj.2014.12.021.

[126] M. Popa, B. C. Ciobanu, L. Ochiuz, J. Desbrieres, C. S. Stan, and C. A. Peptu, 'CONTROLLING THE RELEASE KINETICS OF CALCEIN LOADED

LIPOSOMES FROM CHITOSAN/TANNIC ACID AND CHITOSAN/POLY(VINYL ALCOHOL)/TANNIC ACID HYDROGELS'.

[127] W. Ge, S. Cao, F. Shen, Y. Wang, J. Ren, and X. Wang, 'Rapid self-healing, stretchable, moldable, antioxidant and antibacterial tannic acid-cellulose nanofibril composite hydrogels', *Carbohydr Polym*, vol. 224, Nov. 2019, doi: 10.1016/j.carbpol.2019.115147.

[128] H. Fan, J. Wang, Q. Zhang, and Z. Jin, 'Tannic acid-based multifunctional hydrogels with facile adjustable adhesion and cohesion contributed by polyphenol supramolecular chemistry', *ACS Omega*, vol. 2, no. 10, pp. 6668–6676, Oct. 2017, doi: 10.1021/acsomega.7b01067.

[129] W. Shi *et al.*, 'Tannic acid-inspired, self-healing, and dual stimuli responsive dynamic hydrogel with potent antibacterial and anti-oxidative properties', *J Mater Chem B*, vol. 9, no. 35, pp. 7182–7195, Sep. 2021, doi: 10.1039/d1tb00156f.

[130] C. Wang *et al.*, 'Tannic acid-loaded mesoporous silica for rapid hemostasis and antibacterial activity', *Biomater Sci*, vol. 6, no. 12, pp. 3318–3331, Dec. 2018, doi: 10.1039/c8bm00837j.

[131] N. Ninan, A. Forget, V. P. Shastri, N. H. Voelcker, and A. Blencowe, 'Antibacterial and Anti-Inflammatory pH-Responsive Tannic Acid-Carboxylated Agarose Composite Hydrogels for Wound Healing', *ACS Appl Mater Interfaces*, vol. 8, no. 42, pp. 28511–28521, Oct. 2016, doi: 10.1021/acsami.6b10491.

[132] L. Y. Zheng, J. M. Shi, and Y. H. Chi, 'Tannic Acid Physically Cross-Linked Responsive Hydrogel', *Macromol Chem Phys*, vol. 219, no. 19, Oct. 2018, doi: 10.1002/macp.201800234.

[133] A. G. Tabriz, M. A. Hermida, N. R. Leslie, and W. Shu, 'Three-dimensional bioprinting of complex cell laden alginate hydrogel structures', *Biofabrication*, vol. 7, no. 4, Dec. 2015, doi: 10.1088/1758-5090/7/4/045012.

[134] A. Sharma, C. Verma, S. Mukhopadhyay, A. Gupta, and B. Gupta, 'Development of sodium alginate/glycerol/tannic acid coated cotton as antimicrobial system', *Int J Biol Macromol*, vol. 216, pp. 303–311, Sep. 2022, doi: 10.1016/J.IJBIOMAC.2022.06.168.

[135] X. Wang, T. Hao, J. Qu, C. Wang, and H. Chen, 'Synthesis of thermal polymerizable alginate-GMA hydrogel for cell encapsulation', *J Nanomater*, vol. 2015, 2015, doi: 10.1155/2015/970619.

[136] F. Araiza-Verduzco *et al.*, 'Photocrosslinked alginate-methacrylate hydrogels with modulable mechanical properties: Effect of the molecular conformation and electron density of the methacrylate reactive group', *Materials*, vol. 13, no. 3, Feb. 2020, doi: 10.3390/ma13030534.

[137] S. R. Abulateefeh and M. O. Taha, 'Enhanced drug encapsulation and extended release profiles of calcium-alginate nanoparticles by using tannic acid as a bridging cross-linking agent', *J Microencapsul*, vol. 32, no. 1, pp. 96–105, Feb. 2015, doi: 10.3109/02652048.2014.985343.

[138] N. Khoshnood and A. Zamanian, ‘Development of novel alginate-polyethyleneimine cell-laden bioink designed for 3D bioprinting of cutaneous wound healing scaffolds’, *J Appl Polym Sci*, vol. 139, no. 21, Jun. 2022, doi: 10.1002/app.52227.

[139] Y. He, F. Yang, H. Zhao, Q. Gao, B. Xia, and J. Fu, ‘Research on the printability of hydrogels in 3D bioprinting’, *Sci Rep*, vol. 6, Jul. 2016, doi: 10.1038/srep29977.

[140] E. Sodupe-Ortega, A. Sanz-Garcia, A. Pernia-Espinoza, and C. Escobedo-Lucea, ‘Accurate calibration in multi-material 3D bioprinting for tissue engineering’, *Materials*, vol. 11, no. 8, Aug. 2018, doi: 10.3390/ma11081402.

[141] E. Gómez-Ordóñez and P. Rupérez, ‘FTIR-ATR spectroscopy as a tool for polysaccharide identification in edible brown and red seaweeds’, *Food Hydrocoll*, vol. 25, no. 6, pp. 1514–1520, Aug. 2011, doi: 10.1016/j.foodhyd.2011.02.009.

[142] D. Leal, B. Matsuhiro, M. Rossi, and F. Caruso, ‘FT-IR spectra of alginic acid block fractions in three species of brown seaweeds’, *Carbohydr Res*, vol. 343, no. 2, pp. 308–316, Feb. 2008, doi: 10.1016/j.carres.2007.10.016.

[143] N. P. Chandía, B. Matsuhiro, E. Mejías, and A. Moenne, ‘Alginic acids in Lessonia vadosa: Partial hydrolysis and elicitor properties of the polymannuronic acid fraction’, 2004.

[144] M. A. Federación Latinoamericana de Química. and H. González-Rodríguez, *Revista latinoamericana de química.*, vol. 39, no. 3. [Federación Latinoamericana de Química], 2011. Accessed: Apr. 18, 2023. [Online]. Available: http://www.scielo.org.mx/scielo.php?script=sci_arttext&pid=S0370-59432011000200003&lng=es&nrm=iso&tlng=en

[145] X. He *et al.*, ‘Tannic acid-reinforced methacrylated chitosan/methacrylated silk fibroin hydrogels with multifunctionality for accelerating wound healing’, *Carbohydr Polym*, vol. 247, Nov. 2020, doi: 10.1016/j.carbpol.2020.116689.

[146] H. Fan, J. Wang, and Z. Jin, ‘Tough, swelling-resistant, self-healing, and adhesive dual-cross-linked hydrogels based on polymer-tannic acid multiple hydrogen bonds’, *Macromolecules*, vol. 51, no. 5, pp. 1696–1705, Mar. 2018, doi: 10.1021/acs.macromol.7b02653.

[147] M. Kesti, P. Fisch, M. Pensalfini, E. Mazza, and M. Zenobi-Wong, ‘Guidelines for standardization of bioprinting: A systematic study of process parameters and their effect on bioprinted structures’, *BioNanoMaterials*, vol. 17, no. 3–4, pp. 193–204, Sep. 2016, doi: 10.1515/bnm-2016-0004.

[148] Y. Wu, Z. Y. (William) Lin, A. C. Wenger, K. C. Tam, and X. (Shirley) Tang, ‘3D bioprinting of liver-mimetic construct with alginate/cellulose nanocrystal hybrid bioink’, *Bioprinting*, vol. 9, pp. 1–6, Mar. 2018, doi: 10.1016/j.bprint.2017.12.001.

[149] Z. Li *et al.*, ‘Improvement of cell deposition by self-absorbent capability of freeze-dried 3D-bioprinted scaffolds derived from cellulose material-alginate hydrogels’, *Biomed Phys Eng Express*, vol. 6, no. 4, Jul. 2020, doi: 10.1088/2057-1976/ab8fc6.

[150] K. Markstedt, A. Mantas, I. Tournier, H. Martínez Ávila, D. Hägg, and P. Gatenholm, '3D bioprinting human chondrocytes with nanocellulose-alginate bioink for cartilage tissue engineering applications', *Biomacromolecules*, vol. 16, no. 5, pp. 1489–1496, May 2015, doi: 10.1021/acs.biomac.5b00188.

[151] B. Kaczmarek *et al.*, 'Novel eco-friendly tannic acid-enriched hydrogels-preparation and characterization for biomedical application', *Materials*, vol. 13, no. 20, pp. 1–12, Oct. 2020, doi: 10.3390/ma13204572.

[152] E. Olchowik-Grabarek *et al.*, 'Inhibition of interaction between Staphylococcus aureus α-hemolysin and erythrocytes membrane by hydrolysable tannins: structure-related activity study', *Sci Rep*, vol. 10, no. 1, Dec. 2020, doi: 10.1038/s41598-020-68030-1.

[153] B. Kaczmarek, 'Tannic acid with antiviral and antibacterial activity as a promising component of biomaterials-A minireview', *Materials*, vol. 13, no. 14. MDPI AG, Jul. 01, 2020. doi: 10.3390/ma13143224.

[154] B. Reig-Vano, B. Tylkowski, X. Montané, and M. Giamberini, 'Alginate-based hydrogels for cancer therapy and research', *International Journal of Biological Macromolecules*, vol. 170. Elsevier B.V., pp. 424–436, Feb. 15, 2021. doi: 10.1016/j.ijbiomac.2020.12.161.

[155] G. Irmak, T. T. Demirtaş, and M. Gumusderelioglu, 'Highly Methacrylated Gelatin Bioink for Bone Tissue Engineering', *ACS Biomater Sci Eng*, vol. 5, no. 2, pp. 831–845, Feb. 2019, doi: 10.1021/acsbiomaterials.8b00778.

CURRICULUM VITAE

2013 – 2018	B.Sc., Biomedical Engineering, Pamukkale University, Denizli, TURKEY

WORK EXPERIENCES

Feb 2023 - …	TUBITAK ARDEB 1002-A (222M325) – Researcher, Abdullah Gül Üniversitesi, Kayseri, TURKIYE
Oct 2021 – Oct 2022	TUBITAK BIDEB 2210-C – Researcher, Abdullah Gül Üniversitesi, Kayseri, TURKIYE
2017	TURKKAL KALIBRASYON – Biomedical Engineer/Intern, Kayseri, TURKIYE
2016	ERU GENKOK – Biomedical Engineer/Intern, Kayseri, TURKIYE